



LAWRENCE  
LIVERMORE  
NATIONAL  
LABORATORY

# Nanoporous Gold as a Platform for a Building Block Catalyst

A. Wittstock, A. Wichmann, M. Baeumer

April 11, 2012

ACS Catalysis

## **Disclaimer**

---

This document was prepared as an account of work sponsored by an agency of the United States government. Neither the United States government nor Lawrence Livermore National Security, LLC, nor any of their employees makes any warranty, expressed or implied, or assumes any legal liability or responsibility for the accuracy, completeness, or usefulness of any information, apparatus, product, or process disclosed, or represents that its use would not infringe privately owned rights. Reference herein to any specific commercial product, process, or service by trade name, trademark, manufacturer, or otherwise does not necessarily constitute or imply its endorsement, recommendation, or favoring by the United States government or Lawrence Livermore National Security, LLC. The views and opinions of authors expressed herein do not necessarily state or reflect those of the United States government or Lawrence Livermore National Security, LLC, and shall not be used for advertising or product endorsement purposes.

# Nanoporous Gold as a Platform for a Building Block Catalyst

*Arne Wittstock<sup>2</sup>, Andre Wichmann<sup>1</sup>, Marcus Bäumer<sup>1</sup>*

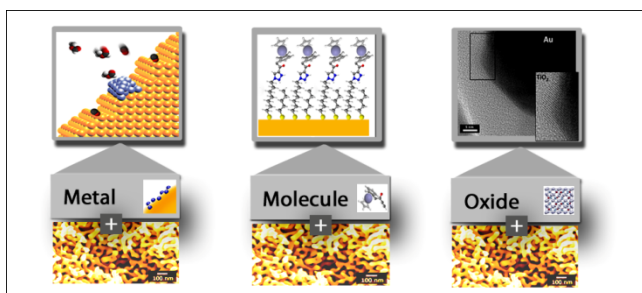
<sup>1</sup> University Bremen, Centre for Environmental Research and Sustainable Technology and Institute of Applied and Physical Chemistry Leobener Strasse NW2, 28359 Bremen, Germany

<sup>2</sup> Lawrence Livermore National Laboratory, NSCL, 7000 East Avenue, CA 94550, USA

## Abstract

Bulk nanostructured materials are of great interest in catalysis as they can be employed in heterogeneous gas and liquid phase catalysis, electro-catalysis and in electro-catalytic sensing. Nanoporous gold gained considerable attraction in this context as it is the prime example of a corrosion derived nanoporous bulk metal. In this review we will summarize recent developments in using this material as the platform for the development of high performance catalytic materials by adding metals, metal oxides and molecular functionalities as building blocks.

## TOC



Keywords: Gold catalysis, nanoporous gold, bimetallic catalyst, gas phase catalysis, electrocatalysis, electro-catalytic sensors

## 1. Introduction to nanoporous gold

Nanoporous gold is a corrosion derived bulk nanostructured material. This material consists of a three-dimensional bicontinuous porous network of interconnected Au ligaments (Figure 1) and pores, respectively. These can be as small as 5 nm, yet, are typically around 30 to 40 nm, depending on the particular preparation procedure. Accordingly, the as-prepared material is mesoporous following IUPAC definition. Due to the high porosity and small feature size, this material is characterized by an extended gold surface with a specific surface area in the range of  $10 \text{ m}^2\text{g}^{-1}$ . The void or pore volume in the resulting material is a function of the concentration of the less noble metal (e.g. Ag or Cu) in the starting compound. Due to fundamental limitations for bulk dealloying, such as the “parting limit” and the stability of the evolving porous network, only alloys containing between about 40 at% and 20 at% Au are viable. Processing of these alloys results in pore volumes between about 60 % and 80 %.

With the onset of nanotechnology in the late 1990s and the beginning 2000s, researchers developed the potential of this material for a variety of technological aspects. The number of publications reporting on nanoporous Au and its technological applications has steeply increased by about 40 percent per year, from about 11 publication in the year 2001 to more than 200 in the year 2011.<sup>1</sup> One of the reasons for the success of this nano-material is its comparatively simple preparation using bench-top corrosion techniques to generate samples in various dimensions (Figure 1). By avoiding financially demanding techniques, as for example electron-beam lithography it became available to a variety of research groups starting to work on the optical or mechanical properties, the catalysis or the electrochemistry of this material.

A broad range of applications seems possible because of the structural and chemical flexibility of the material (Figure 1). Depending on the dimensions of the starting material a large variety of sample morphologies and shapes can be realized. Centimeter sized cubes or cylinders, disks or free standing membranes with thicknesses of some hundreds of microns or even thin films with thickness as low as 100 nanometer are available. Independent of the form, all specimens consist of bulk nanostructured gold with pores and ligaments in the sizes of some tens of nanometers, absolutely homogeneous throughout the entire sample. Temperature activated ripening of the nanostructures opens the door to materials with pores and ligaments in the size regime between ~ 30 nm all the way up to micrometers, without losing the typical bicontinuous structure of the material.<sup>2</sup> By using templating techniques, such as slip casting of alloy coated polystyrene beads

and subsequent removal of the template, hierarchical nanoporous Au structures can be generated with relative densities as low as 2 to 3 percent, values comparable to supported nanoparticle catalysts for example.<sup>3</sup> Furthermore, if this material is used in the form of thin films in the order of 100 nm, the material invest is reduced to less than 0.1 mg Au per cm<sup>2</sup>, a number well acceptable for example in fuel cell applications. Thus, even though npAu is a bulk nanostructured material the overall material-invest of this precious metal can be reduced to competitive and economically viable numbers.

Recent research has impressively revealed that the self-contained nanoporous structure opens the doors for fascinating applications in various fields of catalysis, either using it "as prepared" or after modification with additives, such as metals, metal oxides or organic entities.<sup>4</sup> Due to its nanostructure, this material exhibits a very high specific surface area, maximizing the surface to volume ratio and the surface area which is accessible to reactants. Of advantage is also the high electrical and thermal conductivity in conjunction with the well reproducible and tunable monolithic structure. As shown by model studies under ultra-high vacuum conditions<sup>5</sup>, the surface chemistry of Au is very predictable, also minimizing degradation due to corrosion or poisoning by sticking of undesired surfactants.

In this review, we will focus on means to increase the scope of applications by functionalization of npAu with various additives; we will especially highlight options of using the material as a platform for the preparation of novel catalytic materials according to a building block design. (For more detailed information on the catalytic properties of pure npAu, the reader is referred to other recent reviews on this topic, see ref. 6.) We will first introduce the material and its catalytic potential. In the following sections, we will describe recent efforts and reports aiming at modifying the surface of the material for applications in gas phase catalysis, electro-catalysis and as electro-catalytic sensors.

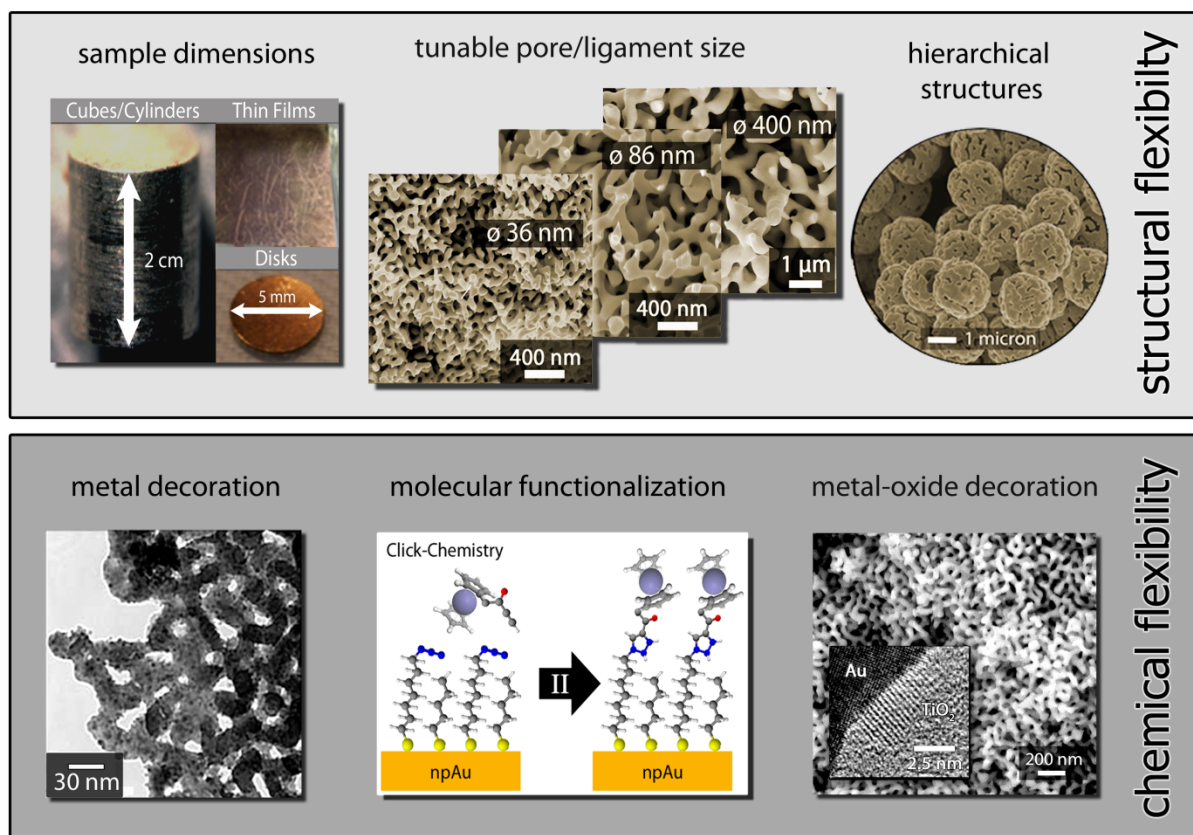


*Figure 1: Structural and chemical flexibility of nanoporous Au based functional materials. Samples with dimensions in the order of centimeters, such as cylinders or cubes, and in the nanometer regime, such as 100 nm thick films, can be readily prepared; pore and ligament sizes can be tailored between several tens of nanometers up to microns. Furthermore, plating techniques open the door to hierarchical structures. Tailoring of the surface chemistry by addition of metals, metal oxides or organic entities enables applications in sensorics and catalysis. (TEM reproduced from ref. 4b, copyright Elsevier (2012)).*

## 1.2 Gold as a material

The famous Greek poet Hesiod described the five ages of mankind in his poem *Works and Days* (~ 700 BC).<sup>7</sup> The first age he names the golden age of mankind, free of the later gradual deterioration of moral values. As a matter of fact, gold was the first metal recognized from humans even before bronze and iron and inspired man kind ever since.<sup>8</sup> The believing in gold as the embodiment of value continued throughout the centuries. Today, the drastically increasing demand of gold as a safe investment very well reflects this fact. One reason for investing in gold

as a safe-haven of treasure and investment is its nobleness and obvious inability to corrode like iron. Gold stays in its metallic form, apparently unaffected by dirt and corrosion. The other reason is that gold is comparatively rare, its average concentration in the earth crust being just 2-5 parts per billion (ppb, weight).<sup>8-9</sup> Only in case of its enriched appearance, such as in the Witwatersrand Basin in South Africa, mining becomes economically viable. The mining of gold strongly profits from the development of production processes to remove the gold from deposits and bringing it into a concentrated and pure form. Today, the largest producer of gold is China with an annual production of 345 t, followed by Australia (255 t) and the United States of America (230 t). Noteworthy, the recycling of gold becomes more and more relevant. In 2010, the U.S. Department of Geological Survey reported that in the U.S. 205 t of gold were generated from recycling of new and old scrap, a number which was even higher than the actual consumption.<sup>10</sup> This reflects that gold is a very sustainable resource.

Most gold is used in the form of jewelry (50 %) or as means of exchange (coins and money) and monetary asset (40 %).<sup>11</sup> The remaining 10 % of the world's gold production goes into the field of industry and technology. Here, it is mostly used in the field of electronics where gold is mainly employed because of its high electrical conductivity and corrosion resistivity.

Yet, gold – as a nanomaterial - also plays an emerging and fascinating role in modern technologies, such as in biomedicine, water purification, fuel cells, exhaust gas purification, energy-efficient glazing coating, touch sensitive screens, even solar cells, and catalysis just to name a few.<sup>11</sup> At first glance, some of these applications seem to contradict the apparent inertness of gold as they involve for example chemical activity of the gold surface. But it is the unique combination of gold and its nanostructure, opening the door for its use in these high-tech applications.

### **1.3 Nanotechnology and gold**

Although the term “nanotechnology” is rather new, the use of nanomaterials can be dated back at least several hundred years ago. First reports on using means of corrosion to generate nanoporous gold can be related to pre-columbian civilizations, such as for example the Incans. Here, the superficial dealloying and subsequent burnishing of a comparably cheaper Au-Cu alloy (removal of the Cu from the alloy surface) was used to generate a shiny gold surface, giving the work piece the allure of pure gold. Undoubtedly, this evoked severe frustration of the Spanish

conquistadores when melting the looted apparently pure gold pieces back in Spain. However, artisans throughout the centuries used this superficial enrichment of Au alloys as a means of gilding. The technique was dubbed depletion gilding or “mis-en-colour”, accordingly.

As mentioned above, a crucial factor for applications of nanoporous gold in catalysis is its nanostructure. The term “nano” or “nanomaterial” implies that critical features and structures of the according material are in the size of several nanometers ( $10^{-9}$  m), typically below 100 nm. This is less than one hundredth of the diameter of a human hair. When dealing with “nano” sized materials new material properties and applications emerge.<sup>12</sup> But why and to what extent should the properties of a material, such as gold, “change” when becoming nano-sized? One important factor is the reduced characteristic length and the increased surface to volume ratio of the materials. When moving from objects with characteristic length-scales (e.g. diameter, edge length) in the order of centimetres or millimetres to the nanometer scale, the surface to volume ratio is increased by a factor of more than one million. The proportion of surface atoms in ligaments (pillars) with diameters in the range of some tens of nanometers is in the order of several percent. They hence constitute a sizable amount of the total number of atoms in the material (Figure 2).



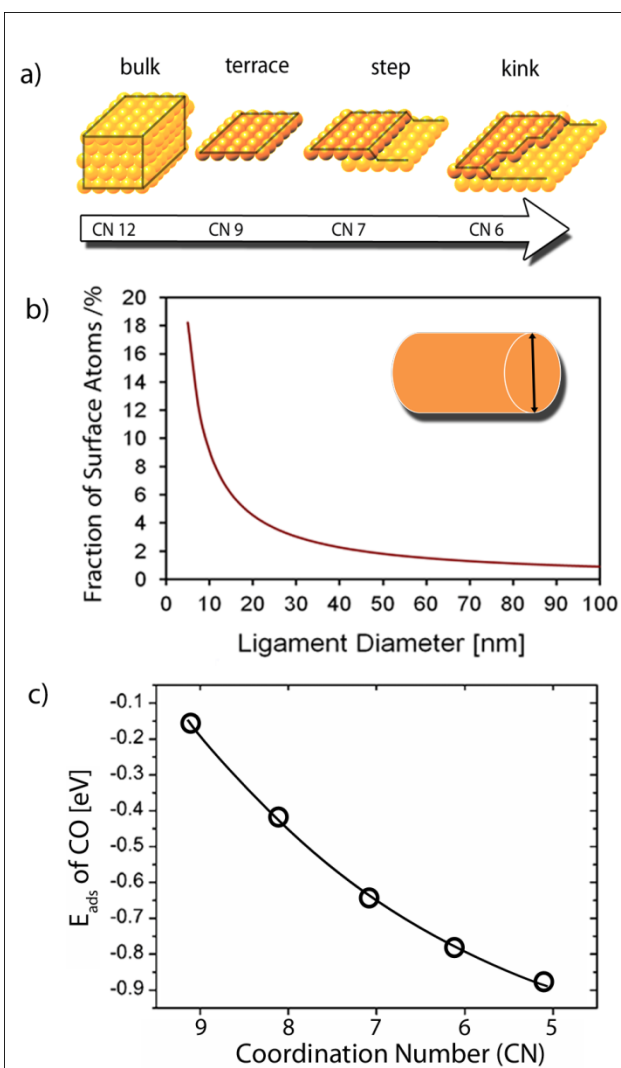


*Figure 2: Characteristics of nanomaterials. A) Surface atoms have a lower number of nearest neighbours (coordination number, CN). B) When reducing the length, such as the diameter of a ligament or pillar, to only nanometers ( $\text{nm} = 10^{-9} \text{ m}$ ), the proportion of surface atoms reaches several, even tens of percent (calculated based on geometric considerations). C) The adsorption and bonding of molecules on the surface is a function of the CN and roughness of the surface, respectively. The energy of adsorption ( $E_{ads}$ ) e.g. decreases (stronger bonding) with decreasing CN (calculated for the adsorption of CO on Au(332) and Au(321); based on ref. 13, copyright of the Royal Society of Chemistry (2012)).*

Nanosized objects are vastly determined by the physicochemical properties of their surface, being distinguished from the bulk properties. In a way, nanosized materials bridge the realm of isolated atoms on the subnanometer scale ( $\text{\AA} = 10^{-10} \text{ m}$ ) and bulk materials. Atoms at the surface have a lower number of neighbouring atoms. Considering a cut through a bulk crystal, the atoms

along this cut have fewer neighbours and accordingly a lower coordination number (CN). Since gold crystallizes in a face centred cubic lattice (fcc), the CN of an atom in the bulk is 12, meaning that every gold atom is surrounded by 12 next neighbours. An Au atom at the surface has a reduced coordination number; depending on whether it is located on a terrace, an edge or a kink site, the CN is reduced to 9, 7, and 6, respectively (Figure 2).

One consequence of the nano-structure is that charge redistribution due to low coordination of surface atoms gives rise to surface stress.<sup>14</sup> The excess charge from unsaturated bonds is redistributed into in-plane bonds which are strengthened or weakened, depending on whether the additional charge is distributed into bonding or antibonding states. Compared to bond lengths of atoms within the bulk, the distance between surface atoms can thus be altered leading to surface stress. In case of compressive stress the surface tends to expand compared to the bulk whereas for tensile stress the surface tends to shrink.<sup>14c</sup> A typical consequence of surface stress is a reconstruction of the surface. Giving an example, the Au(111) surface reconstructs in the commonly known Herringbone reconstruction.<sup>15</sup> The tensile surface stress of the Au(111) surface is compensated by incorporation of about 4 % additional atoms into the surface as compared to the bulk. Recently, several investigations showed that in case of nanoporous metals (npAu, npPt) a change of surface stress can lead to macroscopically detectable strain of the entire material, an effect formerly known for piezo ceramics only.<sup>14a, b, 16</sup>

An additional effect is particularly important for catalysis. The low coordination of surface atoms enhances the reactivity of (metal) surfaces. The desorption enthalpy of CO on gold surfaces is a function of the roughness that is the coordination number of surface atoms (Figure 1.2).<sup>17</sup> Theoretically, there are two ways in which the coordination of a surface atom and the geometry of the surface, respectively, can influence the interaction with molecules and the activation barrier for the reaction; one is electronic and the other one is geometric in origin. The adsorption and bonding of a molecule on a metal surface is determined by the electronic structure of the substrate. A concept describing the interaction (adsorption) of various molecules with transition metals was introduced by Nørskov and co-workers.<sup>18</sup> In transition metals the d-bands determine the reactivity of the substrate as they are the highest lying electronic states. The d-band centre is defined as the first moment (“average”) of the density of d-states. The position (i.e. energy) of the d-band centre with respect to the Fermi level affects the ability of a metal surface atom to form a bond with an adsorbate. For example, transition metal atoms with low

coordination numbers (kink-, edge-sites) tend to have a higher d-band centre. Accordingly, these atoms interact more strongly with adsorbates than atoms in a closed packed surface.<sup>19</sup> Additionally, the geometry of the substrate provides specific adsorption sites which can be crucial for the activation and reaction of the adsorbed molecules.<sup>20</sup> The impact of the latter geometrical effect depends on the transition state, i.e., the optimal local geometry of atoms to form and break bonds. Certainly, the electronic and the geometrical effect are hardly distinguishable, as the local geometry of a surface atom always affects its electronic structure. Yet, both effects contribute to the catalytic performance of a metal. In case of gold the presence of low coordinated atoms even determines whether the surface shows any catalytic activity.<sup>21</sup>

#### 1.4 Generation of Nanoporous Gold

The generation of npAu is based on the electrochemical corrosion of an Au alloy containing one or more less noble constituents. For this reason, this process was dubbed dealloying. Most often used starting alloys are Au-Ag<sup>22</sup>, Au-Cu<sup>23</sup>, Au-Ni<sup>24</sup> and Au-Al<sup>25</sup>, as well as ternary alloys such as Au-Ag(Pt)<sup>26</sup>. More recently, also multi-component bulk metallic glasses have been used.<sup>27</sup> In all these cases, a nanoporous gold material can be obtained, differing though with respect to porosity and composition, owing to differences in the phase diagrams, differences in lattice constants of the alloy constituents, or the different tendencies to passivate during dealloying.<sup>23a, 25</sup> Noteworthy, Au and Ag have both face-centred-cubic (fcc) structures and form a homogeneous solid solution regardless of their composition. Accordingly, corresponding alloys proved to be particularly suitable as they can be dealloyed to > 99 percent<sup>8, 28</sup> (Figure 3) and the resulting porous structure of the npAu is uniform throughout the material (Figure 1).

It turns out that two parameters are crucial for a successful dealloying: the parting limit<sup>29</sup> and the critical potential ( $E_c$ )<sup>30</sup>. The fact that only alloys containing less than ~ 45 at% of Au can be successfully dealloyed is a consequence of this parting limit. This phenomenon can be understood in terms of a coordination effect; above a critical concentration the less noble metal atoms (Ag, Cu) are shielded and passivated, respectively, by Au atoms. Artymowicz et al. recently presented a kinetic Monte-Carlo simulation including the percolation theory.<sup>31</sup> The authors show that the coordination threshold of CN = 9 leads to the experimentally found parting limit of about 55 at%.

Another parameter being important for dealloying is the so called critical potential ( $E_c$ ) which is a consequence of the well-known over-potential in electrochemistry (Figure 3). The Nernst-potential as described by thermodynamics does not suffice to induce bulk corrosion. Only at a potential usually some hundred millivolts higher than the thermodynamic threshold the current resulting from the dissolution of Ag atoms rapidly increases. Investigation of the alloy surface showed that below the critical potential  $E_c$  the resulting surface is smooth and enriched in Au, pointing towards a passivation of the surface due to slow kinetics of Au diffusion.<sup>32</sup> The critical potential  $E_c$  depends on the composition of the starting alloy, the electrolyte, and further additives, such as halides.<sup>30</sup>

An important contribution helping to understand the formation of npAu was the surface diffusion based model developed by Erlebacher and co-workers that is able to reproduce the early stages of the formation of the characteristic 3D morphology of npAu.<sup>12b, 33</sup> This model is based on three competing processes: the electrochemical dissolution of the less noble constituent (Ag), surface diffusion of the noble constituent (Au), and capillary action.<sup>12b, 33b</sup> While the Ag atoms are dissolved in a layer-by-layer fashion, the gold atoms can diffuse along the surface and form islands. Further dissolution of Ag atoms leads to erosion of islands so that ligaments are formed. Due to capillary action, the initially formed ligaments coarsen thus exposing residual silver. Kolluri and Demkovicz recently reported on an atomistic model capturing further stages of the formation of the ligaments of npAu by coarsening of the initial ligament network.<sup>34</sup> Plastic deformation of the initial ligaments by collapsing onto each other drives the coarsening and explains experimental findings such as the minimal ligament diameter of about 5 nm or the observation of voids inside the ligaments<sup>35</sup>.

Basically one can distinguish two means of corrosion: the *free corrosion* and the corrosion in an electrochemical cell, either in a *galvanostatic* or *potentiostatic* manner. In case of free corrosion, the working piece is simply submersed in an electrolyte such as concentrated nitric acid. The open circuit potential drives the dissolution of the less noble material. Free corrosion can be performed at room temperature or even at 0 °C in case of Ag or at slightly elevated temperatures of 40 °C and above in case of Cu and Al.<sup>23a, 25a</sup> This rather simple means of preparation works for thin films in the order of 100 nm up to centimeter sized cubes or cylinders. In case of thin films adhered to a substrate buildup of stress might lead to cracking. Sun and Balk proposed a two-step dealloying approach reducing the overall shrinkage.<sup>36</sup> For larger pieces such

as millimeter sized cubes or disks of  $\text{Au}_{30}\text{Ag}_{70}$ , e.g., alloy shrinkage is typically below 1 % of the edge length and hardly observable.

The second route is dealloying in an electrochemical cell (e.g. *potentiostatic corrosion*) by applying a sufficiently positive potential to the alloy initiating corrosion. Typically, a three electrode setup is used with the alloy piece as working electrode, a reference electrode plus a counter electrode (e.g. a Pt plate). The most commonly used electrolyte is  $\text{HClO}_4$  with concentrations between 0.7 M and 1 M.<sup>37</sup> Another suitable electrolyte is diluted nitric acid, e.g. with a concentration of 5 M<sup>6a</sup> or neutral Ag nitrate solution<sup>38</sup>. The potentiostatic corrosion requires a more sophisticated setup (including a potentiostat) than the free corrosion, but it provides a better control over the corrosion process. For example by applying a slightly higher potential than the critical potential Ag is removed very slowly resulting in mostly crack and stress free npAu films.<sup>37a</sup> At potentials close to the critical potential the corrosion rate is very small, typically in the range of  $\mu\text{A}/\text{cm}^2$ ;<sup>30a</sup> at higher potentials the corrosion is greatly accelerated by about one order of magnitude (cf. Figure 3), reducing the processing time. Especially the high corrosion rate at the very beginning of the dealloying is assumed to induce mechanical stress and the formation of cracks; Okman et al. proposed a step-wise increase of the dealloying potential to solve this issue.<sup>39</sup> For potentials close to the oxidation threshold of Au also smaller ligament and pore sizes are observed, owing to a reduced surface self-diffusion of the Au atoms at this stage.<sup>40</sup> Controlling the potential allows adjusting the dealloying time, the residual Ag, the stress state of the material, as well as the pore size.

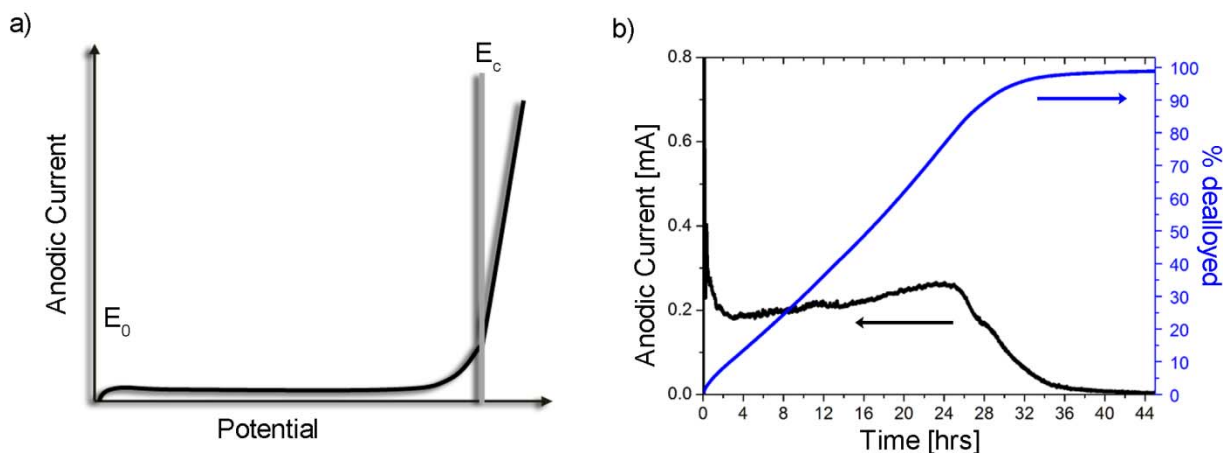


*Figure 3: a) Characteristic run of the anodic current as a function of the applied potential. Above the reversible thermodynamic threshold for corrosion  $E_0$  (e.g. oxidation/dissolution of Ag), the anodic current remains small at first due to a passivation of the alloy surface by Au atoms. Only after reaching the critical potential for bulk corrosion  $E_c$ , the anodic current steeply increases. b) Typical evolution of the anodic current during dissolution of Ag from a  $\text{Ag}_{70}\text{Au}_{30}$  alloy in 5 M nitric acid at 60 mV vs. a Pt reference ( $\sim 1200$  mV vs. NHE under chosen conditions). The anodic current can be transformed into an etching rate. Apparently, after about 32 hours the corrosion of Ag is close to 100 percent and the current approaches zero.*

## 2. Catalysis by Nanoporous Gold

Considering the group of transition metals one can draw a simplistic curve, the so called volcano curve which reflects the potential catalytic activity as a function of the position of the metal in the periodic table of the elements. In this simple picture, the strength of chemisorption (formally the heat of adsorption) decreases with increasing atomic number (i.e. “from left to right”). The bonding of for example oxygen with metal surface such as Ti is too strong as to allow a high enough turn-over. Yet, with increasing atomic number (e.g. from Ti to Cu) the bonding becomes weaker allowing a high enough turn-over, before the chemisorption becomes too weak as to observe appreciable catalytic activity. Accordingly and in agreement with the volcano curve, the highly catalytically active metals can be found in the middle of the row, meaning in the groups 8-10 of the periodic table of the elements (Fe, Co, Ni, Pd, Pt).

Although Au can be found in close neighborhood of these metals, namely in the group 11 (Cu, Ag, and Au) it is distinguished by its nobleness and exceptional weak interaction with adsorbates.<sup>41</sup> First reports on gold as an active catalyst which surprisingly showed that it can be even superior to other metals were published for the hydrogenation of olefines in the 1970s by Bond et al.<sup>42</sup>, later in the mid 1980s for the low temperature oxidation of CO by Haruta et al.<sup>43</sup> and for the chlorination of olefins by Hutchings et al.<sup>44</sup>. Gold was formerly as assumed to be “catalytically dead” due to its apparent inertness, i.e., the weak interaction of gold surfaces with reactants, such as hydrogen or molecular oxygen<sup>41</sup>. Yet, if gold is in the form of very small particles in the range of a few nanometers and deposited on a suitable oxidic support, it may indeed be catalytically highly active. The reason for this kind of behaviour was controversially discussed throughout the last two decades.<sup>45</sup> Especially the chemisorption and activation of molecular oxygen is hardly detectable on pure gold surfaces and strongly profits from the presence of the oxidic support and the nanosized particles.

In 2006 Zielasek et al.<sup>46</sup> and shortly later in 2007 Ding et al.<sup>47</sup> independently discovered that unsupported nanoporous gold is a highly active catalyst for the low temperature oxidation of CO. This finding was unexpected, as npAu is neither made up of nanoparticles nor contains an oxidic support material which was thought to be essential for high catalytic activity so far. At first, it was speculated whether the high abundance of low-coordinated surface atoms within the material is the source of its high catalytic activity revealing the genuine catalytic activity of pure nanostructured but unsupported gold.<sup>47-48</sup> Later reports focused on the remaining traces of the less noble metal, such as Ag, that remain in small quantities below 1 at% in the material after preparation.<sup>49</sup> Since metals such as Ag and Cu, which can be used for generation of npAu, are known to chemically bond and dissociate molecular oxygen, very much in contrast to Au, it is very likely that their presence contributes to the catalytic activity.<sup>13, 50</sup>

Yet, it has to be kept in mind that the origin of the catalytic activity and the active state of the catalysts surface may very well be a function of the surrounding medium as well, being of course different in the gas phase in comparison to reactions in the liquid phase. In the latter case, the surface chemistry and the underlying mechanism are mostly distinguished from the gas phase by a higher concentration of spectator species on the surface. For example, while water can be exploited as a solvent and oxidant in the liquid phase for the oxidation of silanes<sup>51</sup>, its role in the oxidation of CO in the gas phase is very different. Even though it was found to be beneficial for the catalytic activity when in the form of moisture, it cannot be used as the oxidant, replacing O<sub>2</sub><sup>6a</sup>. Nevertheless and in spite of potential contributions of residual components in the material or an influence of the reaction environment, the overall catalytic characteristics of the material in terms of activity and selectivity were found to be governed by the surface chemistry of Au in all cases; for example it was observed that CO oxidation takes place at temperatures well below 0 °C<sup>46</sup> and the highly selective oxidation of alcohols proceeds already at room temperature<sup>28</sup>.

Among other factors, it is the weak interaction with adsorbates that enables high activity at low temperatures making gold a great candidate for predictable and “green” catalytic concepts.<sup>52</sup> The absence of an oxidic support material reduces the degree of complexity regarding the surface chemistry and catalytic properties of npAu. Recent studies showed that insights from well-controllable UHV studies can be directly transferred to npAu catalysts working under ambient pressure conditions.<sup>6a, 28</sup>

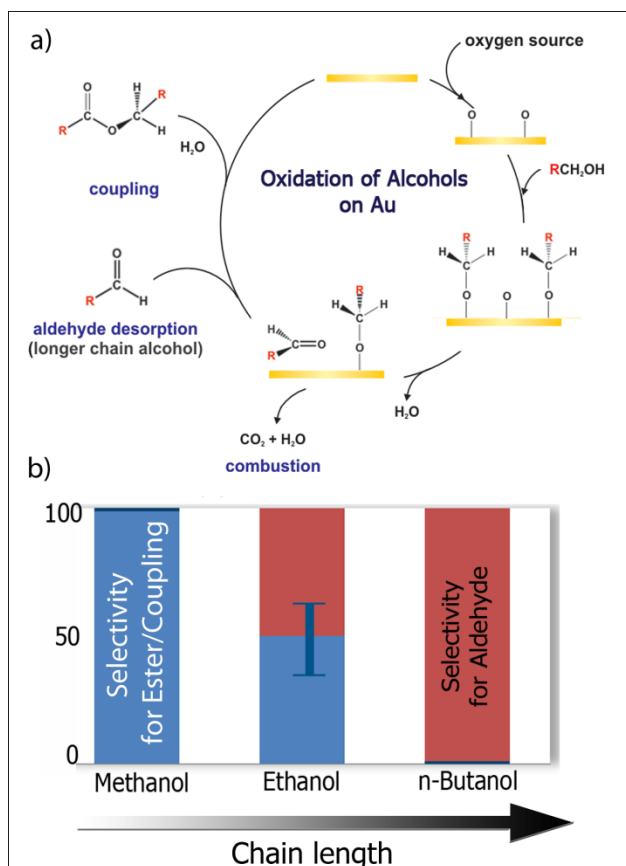


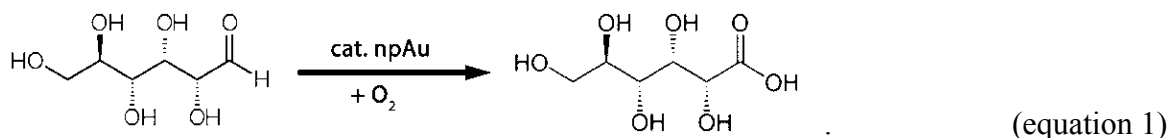
Figure 4: A) Molecular transformation of primary alcohols on npAu in the presence of reactive oxygen.<sup>28, 53</sup> B) The selectivity with respect to either the formation of the ester (coupling) or the aldehyde was found to be a function of the chain length of the alcohol (reproduced from ref.<sup>53a</sup>, copyright John Wiley and Sons (2012)).

For example, the aerobic oxidation of primary alcohols such as methanol, ethanol, and *n*-butanol is catalyzed by npAu already at temperatures as low as 20 °C with considerable yields.<sup>28, 53a</sup> The origin of the catalytic activity of the gold is reactive atomic oxygen adsorbed on its surface.<sup>54</sup> It initiates the catalytic cycle by reaction with the alcoholic proton in a Brønsted acid-base type reaction.<sup>53d, e</sup> The resulting alkoxy group is bonded to the surface and can undergo further  $\beta$ -hydrogen abstraction resulting in the particular aldehyde (Figure 4). The selectivity of the catalytic reaction is governed by the activation energy for  $\beta$ -hydrogen abstraction, resulting in the aldehyde which can either desorb from the surface or react with an adjacent alkoxy moiety forming the ester. Interestingly, this activation barrier is a function of the carbon chain length of the alcohol, decreasing from methanol to ethanol to *n*-butanol.<sup>53c</sup> Accordingly, the selectivity of

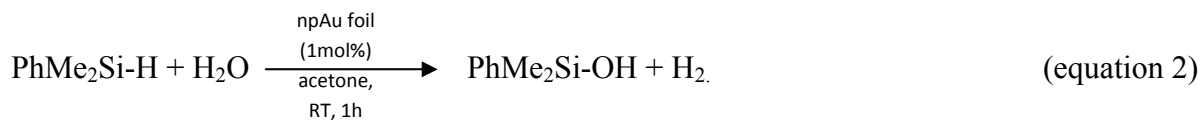


the reaction at ambient pressure when using npAu catalysts was found to shift from the exclusive formation of the ester in case of methanol towards the exclusive formation of the aldehyde in case of *n*-butanol with an intermediate situation of about 50 % conversion into both products in case of ethanol oxidation (Figure 4).<sup>53a</sup> In 2010, Ding et al. reported that also larger alcohols such as benzyl alcohol can be selectively oxidized using npAu catalysts and O<sub>2</sub> as the oxidant.<sup>55</sup> The main product was the industrially important benzaldehyde; the selectivity of the conversion was in all cases above 92 %; the conversion started at temperatures slightly above 200 °C and already at 240 °C the conversion was close to 60 %, showing a remarkable activity (turn-over-frequency of  $\sim 1.4 \text{ s}^{-1}$ ).

Besides these interesting applications of npAu as a catalyst in the gas phase its potential was also demonstrated in liquid phase catalysis. For example, glucose can be selectively oxidized to gluconic acid, employing npAu catalyst at temperatures starting at 30°C and using molecular oxygen as the oxidant<sup>56</sup>:



The reaction conditions were found to be optimal at pH 9 and a temperature of about 60 °C. Importantly, the catalyst could be recycled several times without apparent loss of activity. But not only carbon based compounds can be oxidized using npAu; Asao et al. demonstrated the selective oxidation of organosilanes into the corresponding silanols in water.<sup>51</sup> The authors used 40  $\mu\text{m}$  thin nanoporous gold foil in liquid phase to oxidize various organosilanes. Just giving one example, dimethylphenylsilanol was derived within one hour at room temperature with nearly 100 % yield by using finely dispersed 1 mol% of npAu as a catalyst:



The turn-over-frequency for this reaction was calculated to be about  $3 \text{ s}^{-1}$ . Also in this case, the npAu catalyst could be recycled and reused several (i.e. more than 5) times. It is the remarkable recyclability of the catalyst in conjunction with the stable catalytic activity making this npAu such an interesting material for selective (aerobic) oxidation reactions in liquid phase.

### 3. Combining nanoporous gold with metals

Although the surface chemistry and catalysis of gold leads to impressive activity and selectivity for many chemical reactions, its activity as for example with respect to the oxygen reduction reaction (ORR) being of critical importance in energy related electrochemical applications such as in fuel cells is inferior to highly active metals such as Pt. It is thus tempting to alter and tune the surface chemistry of gold by depositing metals such as Pt, Pd, Ni onto the npAu backbone. The perspective here is twofold: on the one hand, npAu will provide high electrical and thermal conductivity in conjunction with a very high specific surface area; on the other hand, the catalytic activity of a bimetallic system often proves superior owing to a synergistic effect of both metals at the surface resulting in a unique catalytic system.

In the following, we will focus on the modification of npAu by Pt and its applications in liquid phase electro-catalysis with the emphasis on fuel cells as Pt is the most prominent and reactive metal in this context. In addition, we will discuss the use of this material combination for sensor applications, taking the electrochemical detection of glucose as an example.

#### 3.1 Deposition of metals inside the npAu structure

Although it is possible to dealloy trimetallic Au alloys such as Au-Ag(Pt)<sup>26</sup> resulting in bimetallic nanoporous Au-Pt structures, it is economically more favorable to deposit the expensive metal Pt (or Pd) after the formation of the porous network. In general, one can distinguish deposition of metals from the gas phase by physical or chemical vapor deposition and liquid phase deposition by reduction of a metal-salt from solution. In all cases, the high aspect ratio of the pores - i.e., the ratio of the pore diameter and the length of the pore - is a major impediment for uniform and homogeneous coatings of the interior of the porous structure. Techniques such as vapor deposition, comprising evaporation of the metal and subsequent deposition on the porous sample, will inherently suffer from poor conformity of the coating, predominantly leading to a coating of the outer surface of the material. More sophisticated techniques, such as chemical vapor deposition and especially atomic layer deposition (ALD), proved to be advantageous for uniform coatings inside high aspect ratio materials, as shown for example for carbon aerogels with pores in the range of some tens of nanometers, which could be coated with Pt using a well-established ALD routine.<sup>57</sup> Recent work on the deposition of metal

oxides inside nanoporous gold structures using this technique will be discussed later in the according section. An experimentally more facile way of depositing metals uses the reduction of a metal precursor from a surrounding solution by (electro-) chemical means (Figure 5).

The group of Erlebacher et al. developed an electroless plating routine floating thin (i.e.  $\sim 100$  nm thick) npAu sheets (12 karat American white gold leaf) on a water surface containing the particular metal salts and the reducing agent (e.g. hydrazine) in the vapor phase.<sup>58</sup> By separating the two reactants in this way, the reduction primarily proceeds at the gas-liquid interphase and inside the pore volume of the npAu sheet, respectively, thus repressing deposition of the metal on the outer surface. The deposited amount of metal inside the pores can be controlled by removal of the reducing agent at some stage and thus ceasing the reaction. Using  $\text{Na}_2\text{Pt}(\text{OH})_6$  as a precursor salt and hydrazine as a reducing agent, a homogeneous coating with Pt particles inside the npAu structure was obtained after less than 3 hours of reaction (cf. Figure 5).<sup>58</sup> The Pt particles grew epitaxial on the Au substrate and showed a narrow size distribution between 2 nm and 4 nm. The fact that the Pt lattice adapted the slightly larger lattice spacing of the Au substrate, indicates strong bonding between the Pt and the Au substrate.<sup>59</sup> By using this deposition technique, many different metals such as Pt, Pd, Ag, Sn, or even metal oxides such as  $\text{MnO}_2$  can be deposited inside the nanoporous structure.<sup>4a</sup>

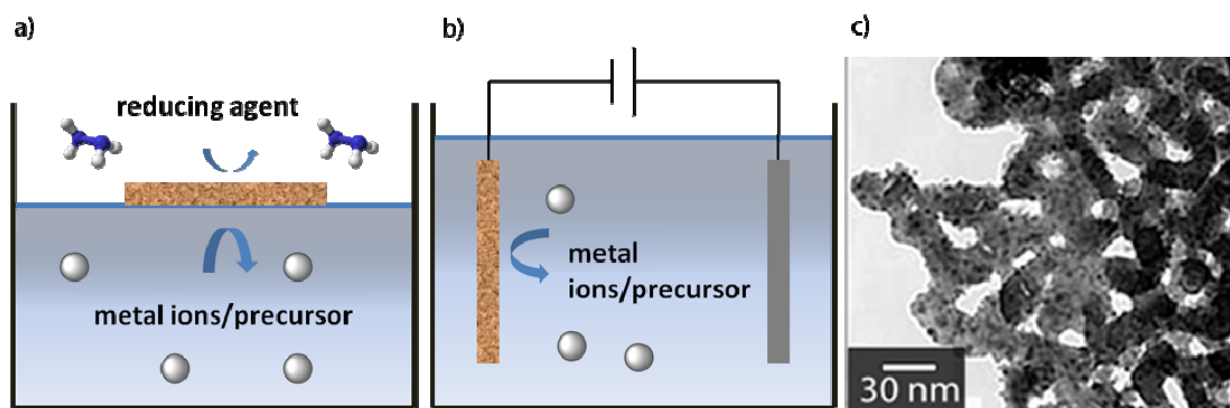


*Figure 5: Deposition of metals by chemical reduction of metal precursors/ions from the liquid phase. a) Chemical reduction at the vapor/liquid interphase b) electrochemical reduction c) transmission electron micrograph of a Pt-npAu composite material prepared by chemical reduction of a Pt salt using hydrazine vapor. The resulting Pt particles are finely dispersed on the Au substrate and have an average size of 3 nm, (reproduced from ref. 4b, copyright Elsevier (2012)).*

A further electrochemical technique to obtain uniform coatings inside the nanoporous structure is under-potential deposition (UPD) (Figures 5b and 6a). By definition, the term UPD denotes deposition of approximately one monolayer of a dissimilar metal A on a metal substrate B at an electrochemical potential more positive/anodic than required for bulk deposition of A.<sup>60</sup> At this potential the deposition of (sub-) monolayer amounts of the ad-metal is thermodynamically favored, for the interaction between the ad-metal A and the substrate B is more favorable than the interaction of A and A. As this method is equivalent to the atomic layer deposition mentioned above, it is also referred to as electrochemical atomic layer deposition. Typical ad-metals which can be deposited on Au substrates are Zn, Ag, Cu, Pb, and Hg; the success and the conformity of the deposited ad-layer, however, strongly depends on the choice of electrolyte, the metal precursor (salt), and the pH.<sup>60-61</sup> Huang et al. investigated the deposition of Zn on npAu substrates using UPD and the subsequent galvanic replacement of the Zn by the more noble Ni metal.<sup>62</sup> The npAu substrate was first submersed in a 0.1 M NaClO<sub>4</sub> electrolyte containing 30 mM Zn(ClO<sub>4</sub>)<sub>2</sub>. At a potential of -394 mV and -307 mV vs. SCE (saturated calomel electrode) stripping of about 1 ML of Zn onto the npAu substrate was observed. In a second step the first deposited layer of Zn was replaced by Ni by submersing the sample in a 50 mM NiSO<sub>4</sub> solution for 3 minutes. The resulting Ni-npAu electrode was tested for oxidation reactions such as glucose oxidation showing about 60 times increased activity as compared to a bare npAu electrode and a larger potential window for electro-oxidation.<sup>62</sup> In a separate study, Rettew et al. investigated the replacement of sacrificial Ni layers deposited on flat and single crystalline Au substrates which were subsequently replaced by Pt by galvanic exchange-reaction (Figure 6).<sup>63</sup> So far, many studies focused on the deposition of for example Cu as the first sacrificial layer due to its advantageous UPD properties; however, Ni can be overpotentially deposited in a very controlled fashion and it is less noble than Cu so that it can be replaced by metals such as Mo, Sn, and Pb in the subsequent galvanic reaction which would not be possible using for example Cu for its electrochemical nobility. To demonstrate the feasibility of this approach even for highly porous electrode materials, a npAu membrane (diameter of 5 mm and thickness of 250  $\mu$ m) was decorated with Pt following Ni deposition according to the procedure described in ref.<sup>63</sup> (cf. Figure 6).<sup>64</sup>

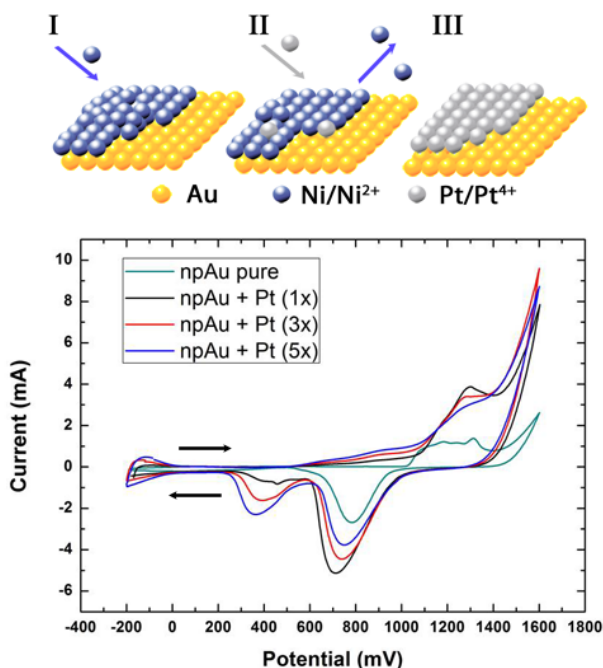


Figure 6: Electrochemical modification of npAu. Upper section: At first a sacrificial Ni layer can be deposited in a very controlled fashion which is subsequently replaced by Pt by galvanic replacement. Lower section: Cyclovoltammograms after each cycle of Pt deposition onto a npAu electrode. First the surface of the npAu electrode was cleaned by cycling the sample in 0.1 M sulfuric acid (green line, no Pt-signal at ~400 mV); subsequently, Ni was deposited by stripping of Ni from a 10 mM  $\text{NiSO}_4$  solution at a potential of -0.9 V vs. Ag/AgCl for 60 seconds. The sample was subsequently immersed in a 10 mM  $\text{H}_2\text{PtCl}_6$  solution for 3 minutes. Cyclovoltammograms of the resulting electrodes for various repetitions of this procedure are displayed. After 5 iterations the signal intensity saturates, indicating complete exchange of the Ni by Pt. (conditions: npAu disk: 5 mm diameter and 250  $\mu\text{m}$  thick; 50 mmol  $\text{H}_2\text{SO}_4$ ; Ag/AgCl reference electrode; sweep velocity of 1 mV/s).<sup>64</sup>

### 3.2 Applications in Fuel Cells

Fuel cells are electrochemical devices generating electricity from a chemical (redox-) reaction. Prominent examples are the so called polymeric-electrolyte- or proton-exchange membrane fuel cells (PEMFC).<sup>65</sup> For low temperature applications (i.e. below 100 °C)  $\text{H}_2$ -PEMFCs and well as the direct methanol fuel cells (DMFC) and direct formic acid fuel cell (DFAFC) have been widely investigated.<sup>65</sup> While for all of these cells oxygen is reduced on the cathode side of the cell (oxygen reduction reaction = ORR), the anodic oxidation reaction is based on the splitting and oxidation of the particular fuel ( $\text{H}_2$ , methanol, formic acid). Pt is typically employed as the catalytically most suitable metal on both electrodes, finely dispersed on a conductive support. Carbon type supports (carbon black, activated carbon or carbon aerogels<sup>57, 66</sup>) are preferable in terms of their economic viability and the low cost of carbon as a resource.

Fast degradation of carbon based systems due to the lack of a chemical interaction of the Pt particles with the carbon support, as well as corrosion and fast contamination of the carbon support inspired further research on alternative strategies.

Interestingly, Pt-npAu as a highly conductive, durable, and active electrode material –profiting from a bimetallic effect enhancing the catalytic activity - can achieve economic viability when in the form of very thin films requiring less than 0.1 mg of Au and 50  $\mu\text{g}$  of finely dispersed Pt per  $\text{cm}^2$ .<sup>4b</sup> In the following, we will report on Pt decorated npAu electrode materials with respect to the oxidation of  $\text{H}_2$ , methanol and formic acid, respectively and their application in fuel cells.

Erlebacher et al. investigated the integration and the activity of Pt-npAu electrode material in  $\text{H}_2$ -PEMFC. They employed the chemical reduction of a Pt salt by hydrazine inside the pores of a npAu leaf ( $\sim 100$  nm thick) as described in the previous section (cf. Figure 5 a). Following the MEA (membrane electrode assembly) approach, the Pt-npAu leafs were sandwiched on both sides of a Nafion membrane, stabilized by either Teflon treated carbon or stainless steel plates as current collectors. The material thus was employed both as anode ( $\text{H}_2$  oxidation) and cathode material (ORR). Some of the results are displayed in Figure 7. The Pt-npAu PEM cells produced up to 240  $\text{mW}$  per  $\text{cm}^2$  and 4.5  $\text{kW}$  per g of Pt. Overall, the performance of the material was assessed to be very promising. However, further studies have to be carried out to test the practicability of the material especially with respect to handling and stability, i.e. degradation of the catalyst over the duration of weeks and month.

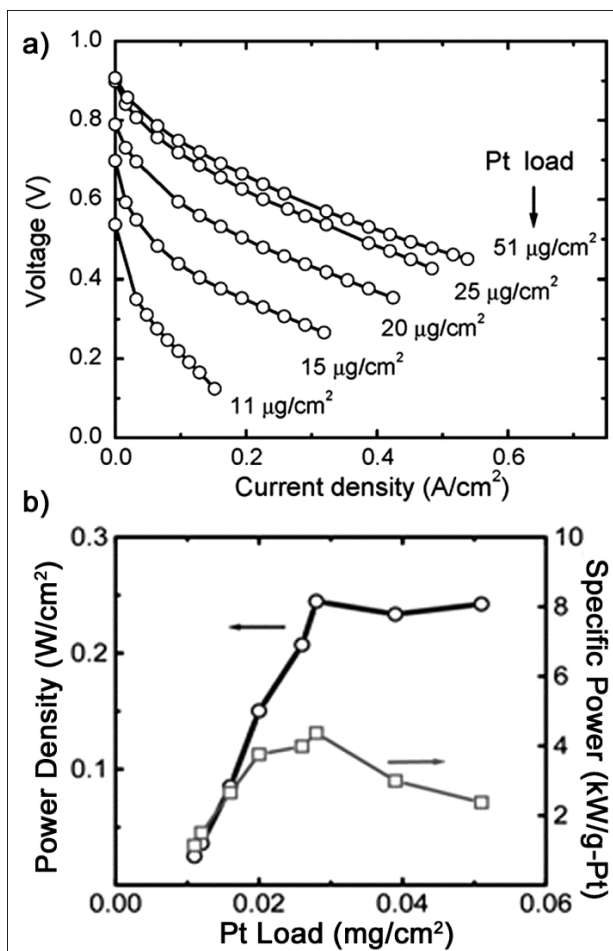


Figure 7: Pt-npAu in a H<sub>2</sub>-PEMFC application. a) Voltage-current polarization curves for different Pt loadings. b) Maximum power density and specific power of Pt-npAu for various Pt loadings. Obviously, a maximal performance is achieved at loadings of around 25 μg Pt per cm<sup>2</sup> (reproduced from ref. <sup>4b</sup>, copyright Elsevier (2012)).

Although fuel cells using hydrogen as fuel are very promising in terms of power density and efficiency, the storage and supply of hydrogen limits their application until now. Especially the storage of hydrogen proved to be very demanding in terms of quantity and leaking issues. Fuel cells circumventing these problems use liquids such as methanol or formic acid as fuel. Methanol (also methyl alcohol or wood alcohol) is a main feedstock for the industrial production of several bulk and commodity chemicals, being produced and thus available in the range of millions of tons per year.<sup>67</sup> Most importantly, methanol is increasingly generated from green and sustainable resources such as from landfill and bio gas. Already in the 1990s the Nobel prize winner George A. Olah advocated methanol as a proper replacement for fossil fuels, proclaiming the methanol economy.<sup>68</sup>

Cyclovoltammograms for the electro-oxidation of methanol in alkaline solution using Pt-npAu electrodes (and uncoated npAu) are shown in Figure 8. The oxidation of methanol on Au and Pt-Au surfaces proceeds at two potentials with different mechanisms. At lower potentials (0-100 mV vs. Ag/AgCl) methanol is oxidized to formate via a four electron transfer:



and at higher potentials ( $> \sim 600$  mV vs. Ag/AgCl) through a 6 electron process to carbonate:



The activity for methanol oxidation strongly depends on the chemisorption and activation of  $\text{OH}^-$  on the electrode surface. The pure npAu electrode lacks activity especially for the oxidation of methanol at low potential. After adding Pt to the Au surface (cf. procedure shown in Figure 6), however, the current is increased by one order of magnitude (Figure 8). The key to this dramatically increased activity is the bi-functional activity involving Au as well as Pt sites on the electrode surface for further oxidation of the carbonyl species (carbonate and formate)<sup>69</sup>, as for example in the following manner:

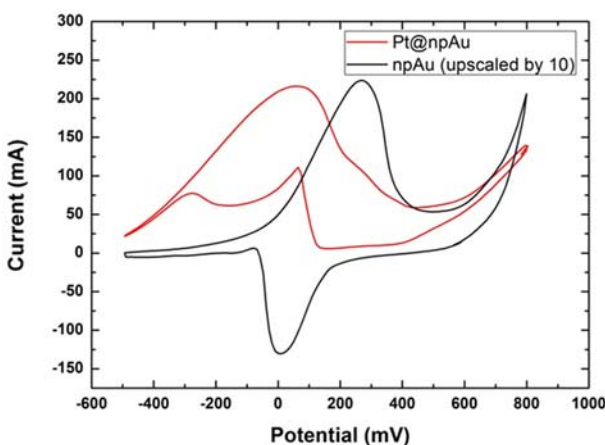


Figure 8: CV curves recorded in 1 M KOH (Riedel-de Haen, p.A.) solution containing 1 M MeOH (VWR, >99.8%). The oxidation signal of the Pt@npAu sample could be increased by one order of magnitude in comparison to the uncoated disk. The oxidation peak on the reverse scan is characteristic for a platinum system (regeneration of active metallic Pt surface based on desorption of  $\text{OH}_{\text{ads}}$  or reduction of Pt



oxides). See in contrast the reduction peak of the pure gold system. (Ag/AgCl reference electrode; scan rate 10 mV/s, npAu disks of 5 mm diameter and 250 microns thickness were used as working electrode).<sup>64</sup>

Problems associated with the use of methanol in fuel cells are related to its high vapor pressure and flammability, as well as with the permeability of the Nafion membrane for methanol leading to an undesired cross over flux.

Formic acid as an alternative fuel proved to be advantageous in this respect allowing for a smaller fuel cell design.<sup>70</sup> Industrially, formic acid is derived from the oxidation of methanol in the order of millions of tons and is thus readily available.<sup>71</sup> As the oxidation state of formic acid is higher than that methanol, its power density is only 1740 W·h/g. Yet, for the above mentioned reasons one can run formic acid fuel cells with higher concentrations of the fuel (e.g. 70 wt%) compensating the lower power density. In addition, the electrochemical driving force in DFAFCs is higher, theoretically allowing open circuit potentials of about 1.45 V.

According to Behm and co-workers, the oxidation of formic acid on Pt surfaces in an acidic environment generally proceeds via an indirect dehydration pathway (equation 6), a formate pathway, or a direct dehydrogenation process (equation 7)<sup>72</sup>:



The important difference between these mechanisms is the formation of intermediates such as CO which is known to strongly bond and thus potentially poison active sites on the Pt surface. At low potentials (i.e. 0.2 V vs. RHE) the oxidation of CO on the Pt surface proceeds very slowly inhibiting the conversion of formic acid at potentials below 0.6 V.<sup>72</sup>

Infrared spectroscopic results on bimetallic Au-Pt surfaces indicate that the mechanism based on the direct dehydrogenation (equation 7) is promoted.<sup>73</sup> Accordingly and similar to the case of electro-oxidation of methanol, Pt-npAu electrodes can have superior catalytic activity due to a bimetallic synergistic effect. Wang et al. succeeded recently in the fabrication of a highly active and stable Pt-npAu catalyst employing a sandwich design.<sup>73</sup> First a layer of Pt was deposited on a npAu electrode (npAu-Pt) and subsequently different amounts of Au in the form of small island were deposited on the npAu-Pt electrode (Figure 9). Even very small amounts of Au greatly enhanced the activity of the catalyst for the favourable dehydration of formic acid at low potentials. In addition the durability of the electrode could be considerably enhanced by combining both metals (Figure 9). This electrode design has three very favourable characteristics: it needs very low Pt loadings, exhibits a great tolerance against CO poisoning

and shows a superior stability/durability as compared to Pt/C electrode. Based on in-situ infrared spectroscopic characterization, Wang et al. concluded that the direct oxidation of formic acid (equation 7) at low potentials, indeed, greatly favours from the presence of Au and isolated Pt atoms on the surface.<sup>73</sup>

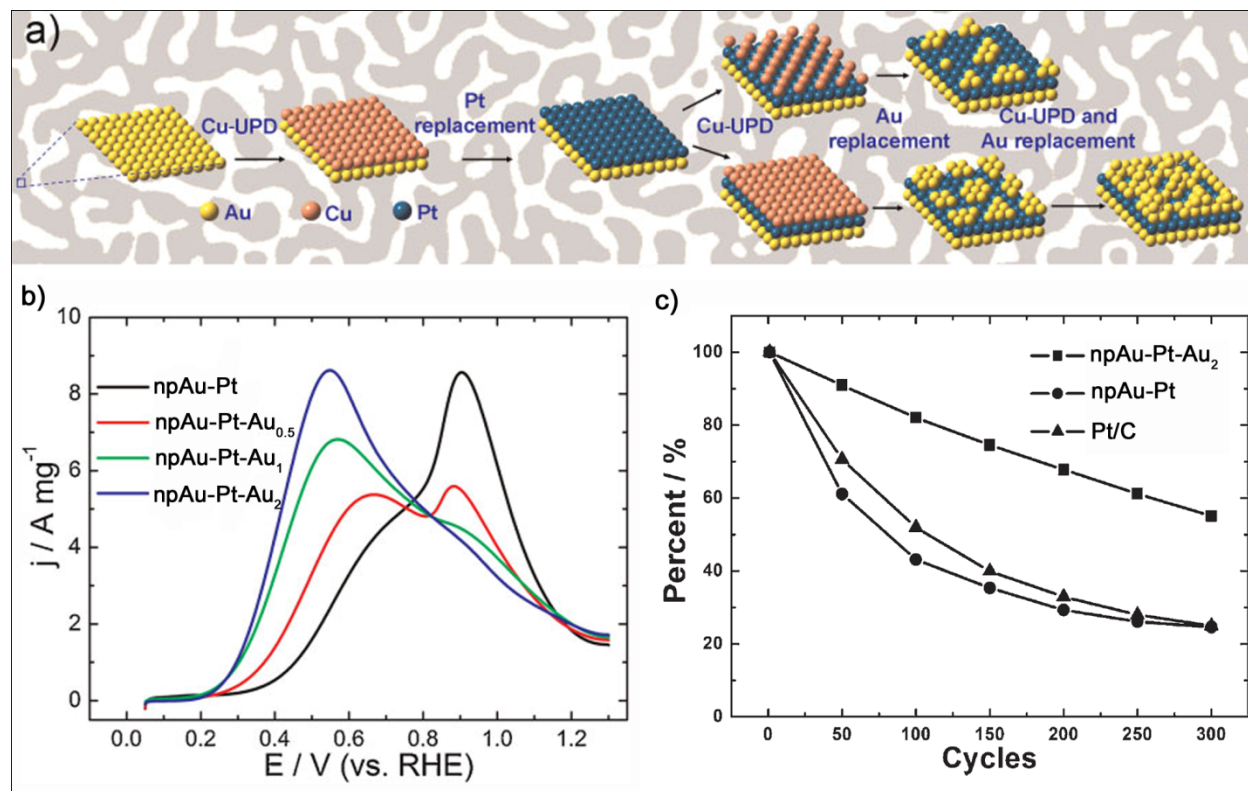


Figure 9: Electro-oxidation of formic acid using Pt-npAu electrodes. a) Schematic illustration of the fabrication procedure of NPG-Pt<sub>1</sub>-Au<sub>x</sub> catalysts. b) Oxidation of formic acid: CV segment of the forward scan of npAu-Pt<sub>1</sub>-Au<sub>x</sub> catalysts in 0.1 M HClO<sub>4</sub> and 0.05 M HCOOH. c) Loss of activity of npAu-Pt, npAu-Pt-Au and a commercial Pt/C electrode material after extensive cycling in 0.1 M HClO<sub>4</sub> between 0.05 and 1.5 V (reproduced from ref.<sup>74</sup>, copyright Wiley and Sons (2012)).

### 3.3 Pt modified npAu for electro-catalytic sensing

NpAu electrode materials offer very high surface areas combined with high catalytic activity and durability. As a consequence they are especially suitable as highly sensitive electrochemical sensors. The working principle of an electrochemical sensor is based on the selective catalytic reaction of a probe molecule. The associated current works as the sensing signal. Several studies during the last years demonstrated the large potential of npAu electrodes for sensing (detection

and quantification) of various important biological substances, such as glucose<sup>4a, 56, 75</sup>, dopamine (DA)<sup>76</sup>, ascorbic acid (AA)<sup>76</sup>, hydrogen peroxide (H<sub>2</sub>O<sub>2</sub>)<sup>77</sup> and NADH<sup>78</sup>. In the context of this review, we will focus on glucose as it is a prime biomolecule and the main source of energy for the human body. Its sensing is of practical importance in the context of medical diagnosis, but also in fermentation and food production processes, e.g. in the production of wine. Common sensors use enzymes as the sensitive “antenna” for glucose detection and the metal electrode as current collector. However, these sensors are prone to fast deactivation and loss of activity as a consequence of the degradation of the enzyme.<sup>79</sup> Novel sensor materials which combine high sensitivity and selectivity in the detection of glucose and appreciable durability are of great interest. Suitable electrode materials typically comprise precious metals such as Au, Pt, Pd, Ag, and their alloys.<sup>80</sup> In this context Huang et al. studied npAu and Pt modified npAu electrodes for glucose sensing (Figure 10).<sup>75b</sup> The sensing of the electrode material in neutral media is based on the electro-oxidation of glucose to gluconolactone at potentials between 0.2 and 0.4 V (vs. standard calomel electrode (SCE)).<sup>81</sup> The oxidation of glucose was studied under neutral pH (phosphate buffer saline, pH 7.4) as this mimics physiological conditions, e.g., in human blood. The npAu type electrode material showed a more than 100 times increased current as compared to a smooth Au electrode owing to its roughness and high surface area. As in the case of methanol or formic acid oxidation the activity could be increased by adding small amounts of Pt onto the Au surface. If the Pt coverage did not exceed 60 %, the Pt-npAu electrode showed an increased activity by about 24 %. At higher coverage the Pt formed 3 dimensional islands on the surface which apparently were less active for the electro-oxidation. Noteworthy under alkaline conditions Pt addition was not beneficial for the catalytic activity. The higher activity of the Pt-npAu electrode materials was attributed to a synergistic effect on the oxidation of glucose.<sup>82</sup> Aside from the high activity and selectivity of the npAu electrode material, its stability was in the focus of the study of Huang et al.. They investigated the CV response during the oxidation of glucose over the period of 1 month (testing every 5 days). The electrode material retained 95 % of its initial activity after this period, indicating a very high stability.

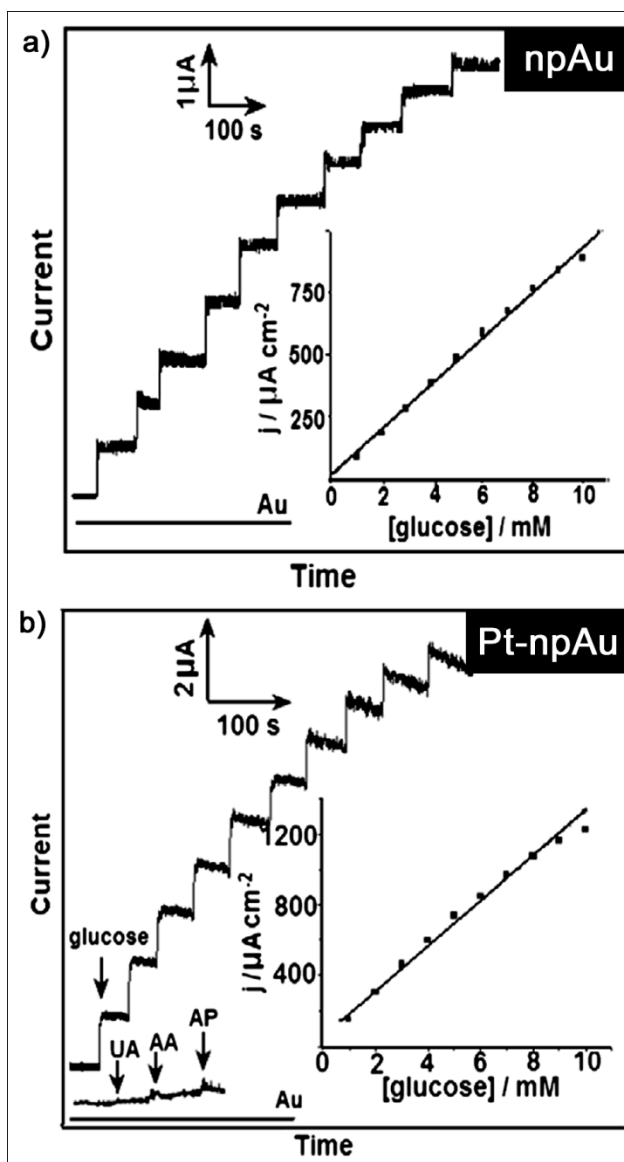


Figure 10: Amperometric detection of glucose using npAu (at + 0.35 V) and Pt-npAu (at + 0.2 V) electrodes. The current vs. time curves were recorded while successively adding 1mM glucose, as well as 0.02 mM uranic acid (UA), 0.1 mM ascorbic acid (AA), 0.1 mM adenosine phosphate (AP); the electrolyte was phosphate buffer saline pH 7.4 containing 0.1 M KCl, hence, mimicking physiological conditions. The insets show the corresponding calibration curves for glucose quantification (reproduced from ref. 75b, copyright Elsevier (2012)).

#### 4 Combining nanoporous gold with organic catalytic entities

A further option of adding a specific functionality to the npAu material is its functionalization by organic catalytic entities generating specific reactivity. Molecules or complexes are chemically immobilized on the npAu substrate so that homogeneous catalysts which are otherwise dispersed in a reaction media can

be turned into a heterogeneous catalyst accompanied with the advantages of a better recyclability, easy separation of the catalyst from the products and reaction media, or electric conductivity for electro-catalytic applications and sensors.

The potential of npAu for this kind of a building block design was demonstrated in several publications during the last about 5 years. Shulga et al. and Qiu et al. demonstrated that npAu is a good carrier for catalysts and biomolecules such as proteins and enzymes.<sup>83</sup> The cornerstone for the immobilization of the molecules is the interaction and bonding of sulfur and nitrogen containing moieties of the biomolecule with the Au surface.<sup>83e</sup> The comparably large pore size of the npAu structure in the range of 30 nm still allows proteins to take their preferred orientation and conformation, respectively, after immobilization; this is of critical importance with respect to their activity. For example, Qiu et al. employed enzyme functionalized npAu for the detection of ethanol and glucose by immobilization of alcohol dehydrogenase and glucose oxidase, respectively.<sup>78</sup> Zhu et al. combined a npAu electrode with cytochrome c preparing a H<sub>2</sub>O<sub>2</sub> sensor working in physiological media.<sup>84</sup> A further very interesting combination is the immobilization of antibodies on the npAu surface as label-free electrochemical immunosensors. Wei et al. demonstrated that an ultrasensitive npAu based immunosensor for the detection of cancer biomarker prostate specific antigen can be prepared by immobilization of an anti-PSA antibody onto the npAu surface.<sup>85</sup> The electro-catalytic oxidation and reduction of K<sub>3</sub>Fe(CN)<sub>6</sub> at the electrode surface could be used as a sensitive reaction towards the formation of the antigen and the specific antibody with very high sensitivity as low as 3 pg/mL of antibody.

In the following we will first report on exemplary chemical means of bonding organic molecules onto the npAu surface. Second we will describe results using functionalized npAu electrodes as sensitive redox-electrodes. In the last section we will describe applications of enzyme modified npAu electrodes in more detail.

#### **4.1 Two-step immobilization of organic entities using click chemistry**

For a stable and reproducible immobilization of an organic molecule onto the npAu surface a chemical bond between the organic molecule and the gold surface is necessary. Although, gold lacks reactivity towards many chemical reactions<sup>41</sup> it exhibits a very selective reactivity towards the bond-formation with some heteroatoms, such as sulfur, nitrogen and chlorine.<sup>15b, 86</sup> Using this specific reactivity of Au for example for the bonding of sulfur was used extensively for the preparation of self-assembled monolayers onto Au substrates.<sup>87</sup> It is thus obvious to use this kind

of chemistry also for the immobilization of catalytically active molecules onto the npAu surface. In order to prevent direct reaction of the catalytically active moiety with the Au surface a two-step approach is most suitable, comprising first the attachment of a layer of linker and spacer molecules and, in a second step, the chemical bonding of the catalytic active molecule to the linker molecules (cf. Figure 11).

The deposition of the first layer of linker molecules works in analogy to the self-assembly of thiol molecules on Au surfaces. In the second step a so-called “click-reaction” can be employed. In 2001 Sharpless and co-workers coined this term for their Cu(I)-catalyzed Huisgen 1,3-dipolar cycloaddition of azides and terminal alkynes forming 1,2,3-triazoles (cf. Figure 11).<sup>88</sup> The resulting triazole rings are chemically exceptionally inert to reactive conditions (e.g. hydrolysis and oxidation). As the click reaction can be used at a wide range of temperatures, pH values, and solvents it is a very suitable and versatile chemical tool for attaching organic entities.

#### **4.2 Highly sensitive redox electrodes**

Following the above described two-step approach for the organic functionalization of npAu, redox-active ferrocene entities can be attached to the npAu surface (Figure 11). For the immobilization of the linker and a diluting thiol (ensuring a sufficient distance between the linker and thus the later attached functionalities on the surface), the nanoporous gold substrate was immersed in a solution containing 50 mM 11-azidoundecane-1-thiol and 150 mM octane-1-thiol (Sigma Aldrich, >98.5%) in ethanol for 3 days (Figure 11b). The subsequent attachment of the electroactive species propynoyl ferrocene was achieved by immersing the npAu-disk in a solution containing 0.25 M propynoyl ferrocene, 0.1 M Cu[TBTA]PF<sub>6</sub> and 0.25 M hydroquinone (Sigma Aldrich, >99.0%) in DMSO (Merck, p.A.)/H<sub>2</sub>O 3:1 for 24 hours. To compare current densities between npAu and a planar system a gold foil was treated precisely the same way (Figure 11c).

Using this two-step approach provides a good control over the formation of the self-assembled monolayer and also avoids a potential direct reaction of a ferrocene group with the Au surface. The resulting ferrocene/npAu system was characterized using cyclic voltammetry (Figure 11c).

Due to its high surface area, the resulting current density (referenced to the geometric surface of the sample) was nearly two orders of magnitude larger than that of a planar Au electrode.

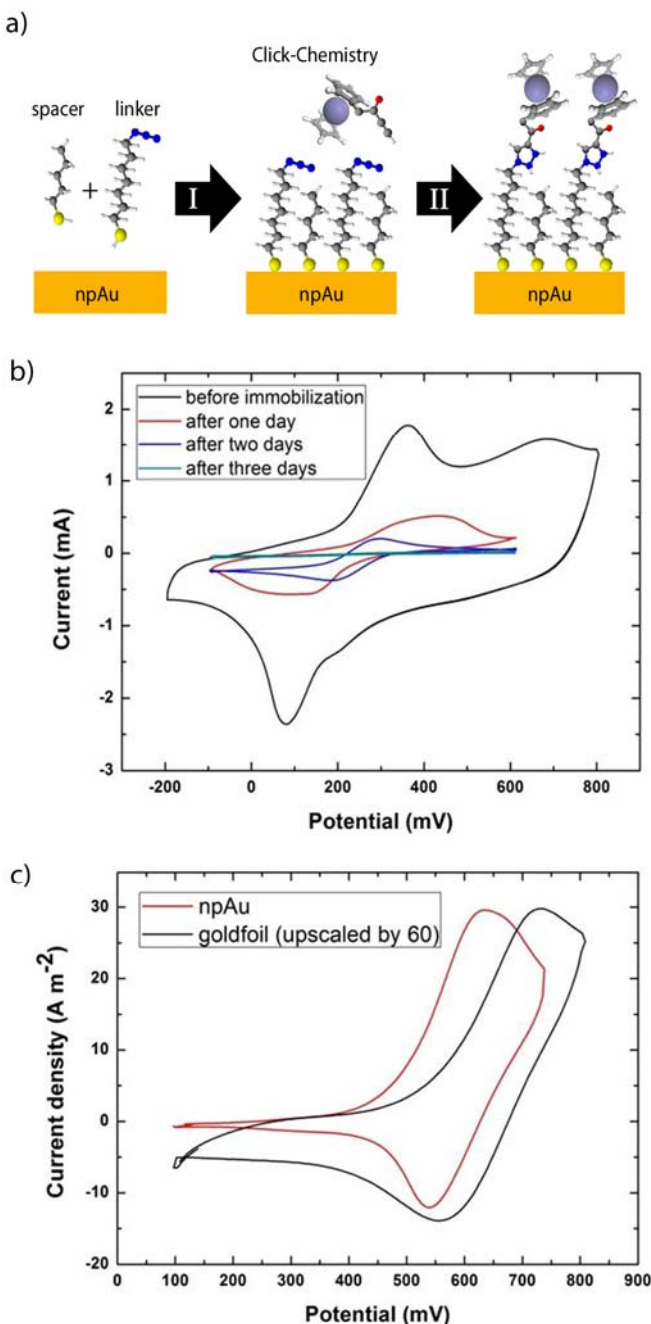


Figure 11. a) Immobilization of a catalytically active functionality onto the npAu substrate. First a monolayer of thiols working as a “linker” is deposited by self assembly. In a second step the desired functionality (here ferrocene) is bonded to the first linker by a click chemistry. b) Cyclic voltammograms



(CV) after linker immobilization (step I). The CVs were measured in 0.1 M KCl (ACROS, p.A.) with 5mM  $K_3Fe(CN)_6$  (Merck, p.A.) vs. Ag/AgCl and a scan rate of 10 mV/s. The redox reaction of ferrocene on the npAu surface was used to monitor the degree of coverage of the Au surface by the linker. The absence of any current after three days indicates that the entire surface is covered by the linker molecules. c) Cyclic voltammogram of propynoyl ferrocene clicked to the linker adsorbed on the nanoporous gold and a planar gold foil substrate (step II). The current density of the npAu electrode is higher than for the planar electrode by a factor of 60. The CVs were measured in 0.1 M  $HClO_4$  (Sigma Aldrich, ACS reagent 70%) vs. a Ag/AgCl electrode with a scan rate of 10 mV/s.<sup>64</sup>

### 4.3 Enzyme modified sensors

Biomolecules such as enzymes are biological catalysts. Humans as well as every other living organism on earth rely on these molecules for selectively catalyzing chemical reactions in our body. In terms of selectivity, enzymes are the role model of a catalyst. The combination of enzymes as the catalytically active “antenna” and the npAu as high surface area, biocompatible, and conductive substrate is thus very promising.

Qiu et al. developed a biocatalytic-sensor based on the combination of npAu and enzymes for the detection of alcohols such as ethanol and glucose.<sup>78</sup> They prepared a nanoporous gold electrode from Au-Ag alloy leaf attached to a polished glassy carbon electrode (GCE) working as backbone. For detection of the alcohols the npAu-GCE electrodes were coated with glucose oxidase (GOD) and alcohol dehydrogenase (ADH), respectively. To prevent fast degradation and leakage of the enzymes the npAu/enzyme electrodes were bedewed with a cation exchange polymer (Nafion). The Nafion/ADH-npAu/GCE catalyst showed a linear response in the amperometric current-time curve over the ethanol concentration range of 1–8 mM with a sensitivity of  $0.19 \text{ mA mM}^{-1}$  and a detection limit of 120 mM of ethanol. In a similar fashion, the Nafion/GOD-npAu/GCE responded linearly to glucose concentration in the range of 1–18 mM with a sensitivity of  $0.049 \text{ A mM}^{-1}$  and a detection limit of 196 mM of glucose. Particularly important is the good stability of the npAu/enzyme electrode-sensors; the authors detected a loss of activity of as little as 5 % over the duration of one month.

A further enzyme modified sensor in combination with npAu was developed by Zhu et al. in the form of an encapsulated cytochrome c (cyt-c) npAu electrodes for  $H_2O_2$  sensing.<sup>89</sup> Different than described in the previous section about the preparation of npAu, in this contribution the authors



used a different procedure for generation of the nanoporous gold electrode. As the starting material Zhu et al. prepared an assembly of Au and Ag nanoparticles using a linker molecule (1,5-pentanedithiol). In the next step the Ag was leached out of this Au-Ag-particle assembly by galvanic replacement of Ag atoms by Au from a  $\text{HAuCl}_4$  solution at room temperature. As one  $\text{Au}^{3+}$  ion leaches three Ag atoms the resulting structure consists of a nanoporous and rough gold surface. After preparation of the npAu electrode it was coated with a solution of the enzyme (cyt-c) and dried. The integrity of the enzyme after immobilization was monitored by UV/VIS spectroscopy. The major absorption wavelength of cyt-c adsorbed on the npAu electrode was only slightly red-shifted (from 409 nm to 411 nm), indicating that no denaturation of the enzyme occurred during immobilization and the conformation of the immobilized enzyme was still intact. This finding also reconfirms the good biocompatibility of the npAu material. The cyt-c encapsulated npAu bio-electrode responded linearly to  $\text{H}_2\text{O}_2$  concentration range of 10  $\mu\text{M}$  to 12 mM, with a detection limit as low as 6.3  $\mu\text{M}$ . Noteworthy, this biosensor not only showed good biocompatibility but also convincing stability, over the duration of 1 month almost no degradation was detected.

## 5 Combining Nanoporous Gold with Metal Oxides

The combination of npAu with metal oxides for catalytic applications is a very promising approach for several reasons. First, pure gold lacks the ability of efficiently activating molecular oxygen which is the natural source for reactive atomic oxygen. In case of pristine npAu, this obstacle can be overcome by traces of a less noble metal (Ag, Cu) in the material. As shown for gold nanoparticles, highly active oxidation catalysts can be generated by combining gold with metal oxides such as titania or iron oxide.<sup>90</sup> Accordingly, metal-oxides are interesting additives, possibly leading to even more active and stable npAu oxidation catalysts. Second, nanostructured metals are prone to temperature activated rippling and coarsening of structures, limiting the applicability at high temperatures. Especially in case of gold the inherent instability of the nanosized structure leads to fast deactivation at elevated temperatures. Biener et al. recently demonstrated that by coating npAu with for example  $\text{Al}_2\text{O}_3$  the nanostructure of npAu can be conserved even at temperatures up to 1000 °C while ligaments in pure npAu start coarsening already at temperatures of about 200 °C.<sup>91</sup>

In general, two different means of deposition of metal oxides into the nanoporous structure of npAu are possible: A) deposition from the gas phase e.g. by chemical or physical vapor deposition techniques (ALD, CVD, PVD) or B) deposition from liquid phase, meaning by dipping of npAu samples into a solution containing either the metal oxide or a viable precursor. In the following, we will report on two examples showing how the modification of npAu with metal oxides can lead to highly active and stable catalysts. Obvious choices for additives are reducible metal oxides such as  $\text{TiO}_2$ ,  $\text{CeO}_2$  or  $\text{FeO}_x$  as these materials are known to lead to high activity in case of gold nanoparticle based systems.

### 5.1 Gas-Phase Deposition: CVD Modified Nanoporous Gold

Chemical - or more specifically - atomic layer deposition (ALD) was shown to be an especially dedicated gas phase deposition technique for the coating of high aspect ratio materials.<sup>57, 92</sup> Already in case of free standing films of npAu with a thickness of 200-300  $\mu\text{m}$  and pore sizes of about 30 nm, the aspect ratio of the pores amounts to several thousands. The slow diffusion of molecules into inner sections of the material is a major obstacle when aiming at homogeneous coating of the inner surface and avoiding clogging of pores close to the outer surface. ALD consists of self-limited surface reactions (i.e. chemisorption) of precursors (cf. Figure 12). This limitation makes ALD an ideally suited technique for such high-aspect ratio materials.

In the first study of this kind, Biener et al. deposited  $\text{TiO}_2$  inside the npAu to generate a highly catalytically active material.<sup>91</sup> Titania was chosen as an exemplary reducible oxide leading to highly active gold based catalytic materials. For deposition, a well-established process using titanium tetrachloride ( $\text{TiCl}_4$ ) and water ( $\text{H}_2\text{O}$ ) was employed.  $\text{TiCl}_4$  exhibits a sufficiently high vapor pressure so that reasonable partial pressures in the gas phase can be realized already at temperatures slightly above 100 °C. The molecule readily reacts (hydrolyzes) with water and hydroxyl groups on the surfaces forming a “ $\text{Cl}_3\text{Ti-O-Au}$ ” layer. Interestingly, although the interaction of water or hydroxyl with Au surface is generally very weak<sup>93</sup> the concentration of these species on the surface is apparently sufficient to generate even closed layers of titania, a fact which is most likely a consequence of the high concentration of water in the air resulting in a condensed layer of water before the sample is introduced into the ALD system. The average growth rate for the  $\text{TiO}_2$  deposition obtained in the above-mentioned study was about 0.07 nm per ALD cycle. Considering the lattice spacing (O-Ti-O unit) of the Ti anatase phase of 0.35 nm

for the (101) plane<sup>94</sup> this corresponds to roughly 1/5 of a monolayer as an equivalent of a closed layer of titania on the surface.

The impact of the titania coating on the catalytic activity for the oxidation of CO was investigated (Figure 12).<sup>91</sup> In this context the aerobic oxidation of CO is a suitable probe reaction in order to assess the ability of the material for catalytic aerobic oxidation reactions in general. Samples which initially had a closed layer of titania did not show any catalytic activity for the CO oxidation. This is not unexpected since titania itself is not an active catalyst for the aerobic CO oxidation at these temperatures and closed layers of thick titania films obviously passivate the surface.<sup>95</sup> However, after annealing the sample at temperatures of about 550 °C prior to catalytic measurements, activity was detected. At these elevated temperatures, the initially amorphous layer of titania transforms into titania crystallites (anatase) and titania as well as Au surface sites are exposed to the reactants (Figure 12).

The activity for CO oxidation (measured at 60 °C) of the titania modified sample was noticeably amplified by a factor of about 5 as compared to the untreated npAu (Figure 12). The enhanced catalytic activity of the TiO<sub>2</sub>/npAu system is likely due to an improved activation of molecular oxygen as this reaction step is anticipated to have the highest activation barrier.<sup>13</sup> Recent work from Yates et al. suggest that the interface between gold and titania plays a key role for the catalytic activity of these systems; here the molecular oxygen can be efficiently activated and CO adsorbed either on Au or on titania sites can react with oxygen located at the interface.<sup>96</sup>

### 5.1 Liquid-Phase Deposition

Other than deposition of metal oxides from the gas phase, it is also possible to deposit either the metal oxide or its precursor by submersing the sample into the corresponding solution, i.e., by simply impregnating the sample. This bench-top technique provides the advantage of a considerably reduced experimental and instrumental demand.

Ding et al. first employed the deposition of TiO<sub>2</sub> particles suspended in ethanol onto npAu membranes in 2009.<sup>4e</sup> Although the majority of particles were larger than the pores and accordingly were only deposited on the very outer surface, the resulting electrode material showed very promising photocatalytic performance. Wittstock et al. employed a comparable technique to generate TiO<sub>2</sub>/npAu composite materials for catalytic gas phase CO oxidation.<sup>50a</sup> Also in this case the majority of particles were likely dispersed onto the outer surface of the

porous membrane, yet, the catalytic activity of this material for CO oxidation was greatly enhanced by about a factor of about 5.

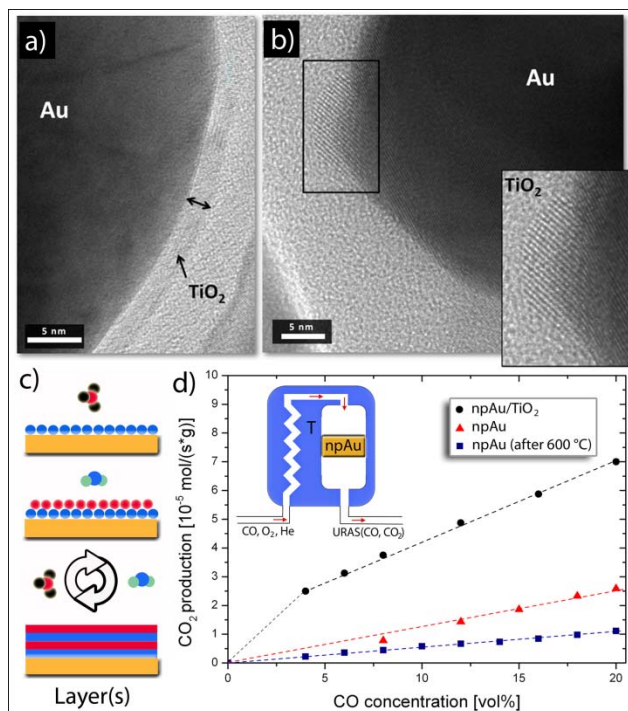


*Figure 12: TiO<sub>2</sub> decorated npAu: a, b) TEM images after heating an ALD coated sample (30 cycles) to 600 °C, the initially closed layer of titania (a) breaks up resulting in titania nanoparticles (b) on the gold surface (scale bars are 5 nm). c) Schematic drawing showing the steps of an ALD deposition. d) Aerobic oxidation of CO at 60 °C using npAu and titania modified npAu (10 cycles) in a continuous flow reactor. (Results for bare npAu sample annealed to 600 °C without titania doping is displayed for comparison; 30 vol% O<sub>2</sub>, Helium as carrier gas, total flow of gases was 50 ml/min)<sup>91</sup>. (TEM, image courtesy of K. Frank and A. Rosenauer, University Bremen, section d) is reproduced from ref. 91, copyright of American Chemical Society (2012))*

Besides direct application of titania particles from a suspensions, TiO<sub>2</sub>/npAu composites can be synthesized using chemical precursors, such as titanium isopropoxide (TTIP). This precursor is a liquid at room temperature so that npAu samples can be simply submersed into it. After calcination at 400 °C in helium finely dispersed coatings of TiO<sub>2</sub> even along the whole cross section of a 300 µm npAu membrane were. The catalytic activity of these TiO<sub>2</sub>/npAu samples for CO oxidation was greatly enhanced as compared to the untreated npAu (Figure 13). Besides being highly active, the nanostructure of the oxide modified npAu system could be preserved at

temperatures as high as 400 °C. As a result of the stabilization of the nanostructure, the TiO<sub>2</sub>/npAu samples showed considerable catalytic durability at high temperatures; for example at 250 °C, the catalytic activity for CO oxidation did not considerably decrease over the period of several days. In a similar attempt this approach can be expanded to other metal oxides such as rare earth oxides. Immersion of a npAu membrane in a solution of Pr(NO<sub>3</sub>)<sub>3</sub> and subsequent calcination to 500 °C lead to deposition of praseodymia particles inside the pores on the npAu surface. In this case the catalytic activity for CO oxidation of the composite material could be amplified, too (Figure 13).

In summary, the combination of the npAu with certain metal oxides results in highly active catalytic materials with superior stability and durability, especially at elevated temperature. Such systems combine high catalytic activity for oxidation reactions at low temperatures, not attained by other precious metal based catalyst, all the way up to several hundred degree Celsius, a favorable characteristic for example in automotive converters, hitherto, an obstacle for gold based catalysts. Noteworthy, by coating the npAu surface with metal oxides a reversed situation as for example opposed to oxide supported metal nanoparticle catalyst is realized. This type of inverse catalyst is a valuable tool for addressing and investigating the interaction between the metal and the oxide.<sup>97</sup> Accordingly, a further more detailed investigation of the systems may also contribute to the mechanistic understanding of Au based catalytic systems in general.

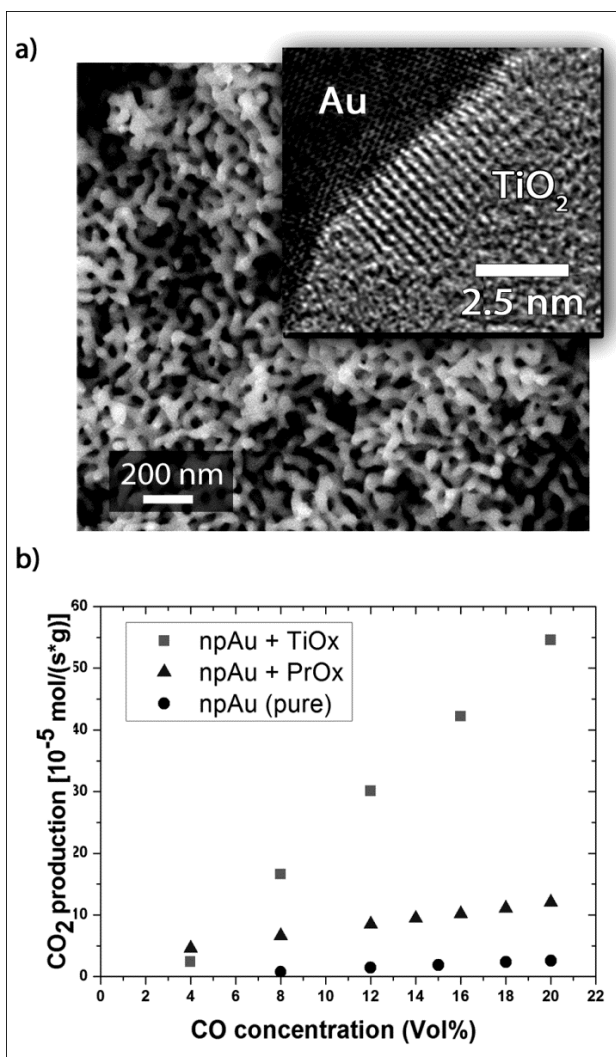


Figure 13: Oxide modified npAu. A) Cross sectional SEM of a titania coated npAu membrane. The sample was first submersed in a TTIP precursor containing solution and subsequently calcined at 500 °C in air. The inset shows a high resolution TEM of a TiO<sub>2</sub> particle on the npAu surface. B) Catalytic conversion of CO using pure npAu and oxide modified npAu at 60 °C (30 vol% O<sub>2</sub> and total flow rate of 50 ml/min).

### Summary and future outlook

In this review we reported on the various aspects of modification of the surface chemistry and catalysis of npAu by introducing metals, metal oxides and molecular catalysts into the porous structure, leading to high performance catalysts for heterogeneous catalysis, electro-catalysis, and electro-catalytic sensing. NpAu is generated by electrochemical means, this is the corrosion of a Au alloy containing at least one less noble constituent such as silver. The particular

advantage of this approach is the broad flexibility with respect to sample dimensions and the comparatively simple preparation by chemical bench-top techniques. Sample dimensions from about 100 nm thick films all the way up to centimeter sized cubes can be generated by simply submersing the corresponding alloy in nitric acid. The resulting mesoporous gold can be employed as a very selective and active catalyst for aerobic oxidation reactions in liquid as well as gas phase catalysis.

However, this electrically conductive and high surface area material also offers a broad range of opportunities for tuning the surface with additives. In the context of electro-catalysis the addition of small amounts of Pt proved to increase the activity of the material. The electro-catalytic reaction of molecules on the catalysts surface can not only be used for energy harvesting such as in fuel cell applications but also for sensing. For example, the current generated by the oxidation of glucose on the npAu electrode surface can be used for quantification and detection of this very important bio-molecule. By adding Pt onto the npAu surface the current response and thus the sensitivity of this sensor can be considerably increased.

In a comparable way, molecular catalysts such as enzymes or metal-complexes can be immobilized and bonded onto the electrically conductive npAu electrode surface. In this way not only the high activity and selectivity of homogeneous catalysts can be implemented into a heterogeneous catalyst but also the current stemming from electro-chemical oxidation reactions can be used for detection and quantification of probe molecules. For example, bio-molecules such as alcohol dehydrogenase and glucose oxidase can be immobilized onto the npAu structure taking advantage of their selectivity with respect to the oxidation of alcohols such as ethanol and glucose.

With respect to heterogeneous gas phase catalysis, the addition of metal-oxides ( $\text{TiO}_2$ ,  $\text{CeO}_2$ ,  $\text{Fe}_2\text{O}_3$  etc.) onto the npAu surface is a very promising route for the generation of highly active and durable catalysts. In analogy to gold nanoparticles which typically have to be deposited on a metal-oxide support to show activity for aerobic oxidation reactions, the addition of a metal-oxide onto the npAu resulted in a considerably increased activity for the aerobic oxidation of CO. In addition to the amplified activity, the oxide modified catalyst showed unprecedented stability at temperatures of several hundred degrees, likely owing to a suppression of surface self diffusion of gold atoms and thus coarsening of the nanostructures by the metal-oxide.

Although humans used this type of nanoporous gold material for centuries in artwork, its



technological applications as for example in catalysis are very young and evolved during the last ten years. For example, the finding that pure npAu is a very active catalyst for aerobic oxidation reactions only dates back about 6 years ago. Within these last years the efforts of several research groups around the world were drawn onto this subject and the applications of this material in many catalytic arenas were investigated. From an applied and economic point of view, further efforts will be necessary to bring nanoporous gold into industrial applications. For example, the material invest, namely the use of a bulk gold material, appears to be an impediment. However, the large flexibility of the material dimensions allows for an intelligent and indeed economically viable application of the material for example in the form of thin films or hierarchical structures. From a scientific point of view, a further investigation and understanding of the catalytic processes on the atomic level will be of great importance. First attempts already proved that the extended gold surface is particularly suited to transfer insights obtained from model studies on Au single crystal surfaces to the catalytic behaviour of npAu under ambient and so called “real-world” catalytic conditions, thus paving the way to a predictable catalyst.

## Acknowledgements

The authors thank the University Bremen and the state of Bremen for financial support. AW's work was performed under the auspices of U.S. Department of Energy by LLNL under Contract DE-AC52-07NA27344.

## References

1. ISIWeb of Knowledge as of June/2011, Keyword "nanoporous gold"
2. (a) Biener, J.; Nyce, G. W.; Hodge, A. M.; Biener, M. M.; Hamza, A. V.; Maier, S. A., Nanoporous plasmonic metamaterials. *Adv. Mater.* **2008**, *20* (6), 1211-1217; (b) Hodge, A. M.; Biener, J.; Hayes, J. R.; Bythrow, P. M.; Volkert, C. A.; Hamza, A. V., Scaling equation for yield strength of nanoporous open-cell foams. *Acta Mater.* **2007**, *55* (4), 1343-1349; (c) Biener, J.; Hodge, A. M.; Hayes, J. R.; Volkert, C. A.; Zepeda-Ruiz, L. A.; Hamza, A. V.; Abraham, F. F., Size effects on the mechanical behavior of nanoporous Au. *Nano Lett.* **2006**, *6* (10), 2379-2382.
3. Nyce, G. W.; Hayes, J. R.; Hamza, A. V.; Satcher, J. H., Synthesis and characterization of hierarchical porous gold materials. *Chem. Mat.* **2007**, *19* (3), 344-346.
4. (a) Ding, Y.; Chen, M. W., Nanoporous Metals for Catalytic and Optical Applications. *MRS Bull.* **2009**, *34* (8), 569-576; (b) Zeis, R.; Mathur, A.; Fritz, G.; Lee, J.; Erlebacher, J., Platinum-plated nanoporous gold: An efficient, low Pt loading electrocatalyst for PEM fuel cells. *J. Power Sources* **2007**, *165* (1),



- 65-72; (c) Biener, M. M.; Biener, J.; Wichmann, A.; Wittstock, A.; Baumann, T. F.; Bäumer, M.; Hamza, A. V., ALD Functionalized Nanoporous Gold: Thermal Stability, Mechanical Properties, and Catalytic Activity. *Nano Lett.* **2011**, null-null; (d) Wittstock, A.; Wichmann, A.; Biener, J.; Bäumer, M., Nanoporous gold: a new gold catalyst with tunable properties. *Faraday Disc* **2011**, 152 (0), 87-98; (e) Jia, C. C.; Yin, H. M.; Ma, H. Y.; Wang, R. Y.; Ge, X. B.; Zhou, A. Q.; Xu, X. H.; Ding, Y., Enhanced Photoelectrocatalytic Activity of Methanol Oxidation on TiO<sub>2</sub>-Decorated Nanoporous Gold. *J. Phys. Chem. C* **2009**, 113 (36), 16138-16143.
5. (a) Liu, X. Y.; Madix, R. J.; Friend, C. M., Unraveling molecular transformations on surfaces: a critical comparison of oxidation reactions on coinage metals. *Chem. Soc. Rev.* **2008**, 37 (10), 2243-2261; (b) Meyer, R.; Lemire, C.; Shaikhutdinov, S. K.; Freund, H., Surface chemistry of catalysis by gold. *Gold Bull.* **2004**, 37 (1-2), 72-124.
  6. (a) Wittstock, A.; Biener, J.; Bäumer, M., Nanoporous gold: a new material for catalytic and sensor applications. *Phys. Chem. Chem. Phys.* **2010**, 12 (40), 12919-12930; (b) Wittstock, A.; Biener, J.; Erlebacher, J.; Bäumer, M., *Nanoporous Gold: from an Ancient Technology to a Novel Material*. 1 ed.; RSC: 2012; Vol. 1, p 250.
  7. Hesiod, A. N. A., *Hesiod; Theogony; Works and days; Shield*. Second ed.; JHU Press: 2004.
  8. Renner, H.; Schlamp, G.; Hollmann, D.; Lüscho, H. M.; Tews, P.; Rothaut, J.; Dermann, K.; Knödler, A.; Hecht, C.; Schlott, M.; Drieselmann, R.; Peter, C.; Schiele, R., Gold, Gold Alloys, and Gold Compounds. In *Ullmann's Encyclopedia of Industrial Chemistry*, Wiley-VCH: Weinheim, 2000.
  9. Frimmel, H. E., Genesis of the world's largest gold deposits. *Science* **2002**, 297 (5588), 1815-1817.
  10. Salazar, K.; McNutt, M. K., MINERAL COMMODITY SUMMARIES 2011. Interior, U. S. D. o. t.; Survey, U. S. G., Eds. USGS: Washington, 2011; pp 66-67.
  11. Council, T. W. G. About Gold. [http://www.gold.org/about\\_gold/](http://www.gold.org/about_gold/).
  12. (a) Biener, J.; Wittstock, A.; Baumann, T.; Weissmüller, J.; Bäumer, M.; Hamza, A., Surface Chemistry in Nanoscale Materials. *Materials* **2009**, 2 (4), 2404-2428; (b) Erlebacher, J.; Seshadri, R., Hard Materials with Tunable Porosity. *MRS Bull.* **2009**, 34 (8), 561-568.
  13. Moskaleva, L. V.; Rohe, S.; Wittstock, A.; Zielasek, V.; Kluner, T.; Neyman, K. M.; Bäumer, M., Silver residues as a possible key to a remarkable oxidative catalytic activity of nanoporous gold. *Phys. Chem. Chem. Phys.* **2011**, 13 (10), 4529-4539.
  14. (a) Biener, J.; Wittstock, A.; Zepeda-Ruiz, L. A.; Biener, M. M.; Zielasek, V.; Kramer, D.; Viswanath, R. N.; Weissmüller, J.; Bäumer, M.; Hamza, A. V., Surface-chemistry-driven actuation in nanoporous gold. *Nat. Mater.* **2009**, 8 (1), 47-51; (b) Weissmüller, J.; Viswanath, R. N.; Kramer, D.; Zimmer, P.; Wurschum, R.; Gleiter, H., Charge-induced reversible strain in a metal. *Science* **2003**, 300 (5617), 312-315; (c) Haiss, W., Surface stress of clean and adsorbate-covered solids. *Reports on Progress in Physics* **2001**, 64 (5), 591-648; (d) Ibach, H., The role of surface stress in reconstruction, epitaxial growth and stabilization of mesoscopic structures. *Surf. Sci. Rep.* **1997**, 29 (5-6), 195-263; (e) Bach, C. E.; Giesen, M.; Ibach, H.; Einstein, T. L., Stress relief in reconstruction. *Phys. Rev. Lett.* **1997**, 78 (22), 4225-4228.
  15. (a) Biener, J.; Biener, M. M.; Nowitzki, T.; Hamza, A. V.; Friend, C. M.; Zielasek, V.; Bäumer, M., On the role of oxygen in stabilizing low-coordinated au atoms. *ChemPhysChem* **2006**, 7 (9), 1906-1908; (b) Min, B. K.; Alemozafar, A. R.; Biener, M. M.; Biener, J.; Friend, C. M., Reaction of Au(111) with sulfur and oxygen: Scanning tunneling microscopic study. *Top. Catal.* **2005**, 36 (1-4), 77-90.
  16. (a) Jin, H. J.; Kurmanaeva, L.; Schmauch, J.; Rosner, H.; Ivanisenko, Y.; Weissmüller, J., Deforming nanoporous metal: Role of lattice coherency. *Acta Mater.* **2009**, 57 (9), 2665-2672; (b) Kramer, D.; Viswanath, R. N.; Weissmüller, J., Surface-stress induced macroscopic bending of nanoporous gold cantilevers. *Nano Lett.* **2004**, 4 (5), 793-796.

17. Yim, W. L.; Nowitzki, T.; Necke, M.; Schnars, H.; Nickut, P.; Biener, J.; Biener, M. M.; Zielasek, V.; Al-Shamery, K.; Kluner, T.; Bäumer, M., Universal phenomena of CO adsorption on gold surfaces with low-coordinated sites. *J. Phys. Chem. C* **2007**, *111* (1), 445-451.
18. Greeley, J.; Norskov, J. K.; Mavrikakis, M., Electronic structure and catalysis on metal surfaces. *Annual Review of Physical Chemistry* **2002**, *53*, 319-348.
19. Norskov, J. K.; Bligaard, T.; Hvolbaek, B.; Abild-Pedersen, F.; Chorkendorff, I.; Christensen, C. H., The nature of the active site in heterogeneous metal catalysis. *Chem. Soc. Rev.* **2008**, *37* (10), 2163-2171.
20. Norskov, J. K.; Bligaard, T.; Logadottir, A.; Bahn, S.; Hansen, L. B.; Bollinger, M.; Bengaard, H.; Hammer, B.; Sljivancanin, Z.; Mavrikakis, M.; Xu, Y.; Dahl, S.; Jacobsen, C. J. H., Universality in heterogeneous catalysis. *J. Catal.* **2002**, *209* (2), 275-278.
21. Falsig, H.; Hvolbaek, B.; Kristensen, I. S.; Jiang, T.; Bligaard, T.; Christensen, C. H.; Norskov, J. K., Trends in the catalytic CO oxidation activity of nanoparticles. *Angewandte Chemie-International Edition* **2008**, *47* (26), 4835-4839.
22. (a) Forty, A. J., Corrosion Micro-Morphology of Noble-Metal Alloys and Depletion Gilding. *Nature* **1979**, *282* (5739), 597-598; (b) Newman, R. C.; Corcoran, S. G.; Erlebacher, J.; Aziz, M. J.; Sieradzki, K., Alloy corrosion. *MRS Bull.* **1999**, *24* (7), 24-28.
23. (a) Kameoka, S.; Tsai, A. P., CO oxidation over a fine porous gold catalyst fabricated by selective leaching from an ordered AuCu<sub>3</sub> intermetallic compound. *Catal. Lett.* **2008**, *121* (3-4), 337-341; (b) Kameoka, S.; Tsai, A. P. In *Oxidation behavior and catalytic property of intermetallic compound AuCu*, Seoul, SOUTH KOREA, May 21-23; Elsevier Science Bv: Seoul, SOUTH KOREA, 2007; pp 88-92.
24. Rouya, E.; Reed, M. L.; Kelly, R. G.; Bart-Smith, H.; Begley, M.; Zangari, G., Synthesis of Nanoporous Gold Structures via Dealloying of Electroplated Au-Ni Alloy Films. *ECS Transactions* **2007**, *6* (11), 41-50.
25. (a) Wang, X. G.; Qi, Z.; Zhao, C. C.; Wang, W. M.; Zhang, Z. H., Influence of Alloy Composition and Dealloying Solution on the Formation and Microstructure of Monolithic Nanoporous Silver through Chemical Dealloying of Al-Ag Alloys. *J. Phys. Chem. C* **2009**, *113* (30), 13139-13150; (b) Zhang, Z. H.; Wang, Y.; Qi, Z.; Zhang, W. H.; Qin, J. Y.; Frenzel, J., Generalized Fabrication of Nanoporous Metals (Au, Pd, Pt, Ag, and Cu) through Chemical Dealloying. *J. Phys. Chem. C* **2009**, *113* (29), 12629-12636.
26. Snyder, J.; Asanithi, P.; Dalton, A. B.; Erlebacher, J., Stabilized Nanoporous Metals by Dealloying Ternary Alloy Precursors. *Adv. Mater.* **2008**, *20* (24), 4883-+.
27. (a) Lang, X. Y.; Guo, H.; Chen, L. Y.; Kudo, A.; Yu, J. S.; Zhang, W.; Inoue, A.; Chen, M. W., Novel Nanoporous Au-Pd Alloy with High Catalytic Activity and Excellent Electrochemical Stability. *J. Phys. Chem. C* **2010**, *114* (6), 2600-2603; (b) Xu, C. X.; Wang, R. Y.; Chen, M. W.; Zhang, Y.; Ding, Y., Dealloying to nanoporous Au/Pt alloys and their structure sensitive electrocatalytic properties. *Phys. Chem. Chem. Phys.* **2010**, *12* (1), 239-246.
28. Wittstock, A.; Zielasek, V.; Biener, J.; Friend, C. M.; Bäumer, M., Nanoporous Gold Catalysts for Selective Gas-Phase Oxidative Coupling of Methanol at Low Temperature. *Science* **2010**, *327* (5963), 319-322.
29. (a) Tammann, G., The chemical and galvanic characteristics of compound crystals and their atomic distribution - An article on the understanding of alloying. *Z. Anorg. Allg. Chem.* **1919**, *107* (1/3), 1-239; (b) Masing, G., Re-crystallisation of metal. *Naturwissenschaften* **1923**, *11*, 413-422.
30. (a) Dursun, A.; Pugh, D. B.; Corcoran, S. G., Probing the dealloying critical potential - Morphological characterization and steady-state current behavior. *J. Electrochem. Soc.* **2005**, *152* (2), B65-B72; (b) Dursun, A.; Pugh, D. V.; Corcoran, S. G., A steady-state method for determining the dealloying critical potential. *Electrochemical and Solid State Letters* **2003**, *6* (8), B32-B34; (c) Dursun, A.; Pugh, D. V.; Corcoran, S. G., Dealloying of Ag-Au alloys in halide-containing electrolytes - Affect on critical potential and pore size. *J. Electrochem. Soc.* **2003**, *150* (7), B355-B360.

31. Artymowicz, D. M.; Erlebacher, J.; Newman, R. C., Relationship between the parting limit for dealloying and a particular geometric high-density site percolation threshold. *Philos. Mag.* **2009**, *89* (21), 1663-1693.
32. (a) Pickering, H. W., Characteristic features of alloy polarization curves. *Corrosion Sci.* **1983**, *23* (10), 1107-1109, 1111-1120; (b) Pickering, H. W.; Swann, P. R., Electron Metallography of Chemical Attack upon Some Alloys Susceptible to stress Corrosion Cracking. *Corr.* **1963**, *19*, 373t.
33. (a) Erlebacher, J., An atomistic description of dealloying - Porosity evolution, the critical potential, and rate-limiting behavior. *J. Electrochem. Soc.* **2004**, *151* (10), C614-C626; (b) Erlebacher, J.; Aziz, M. J.; Karma, A.; Dimitrov, N.; Sieradzki, K., Evolution of nanoporosity in dealloying. *Nature* **2001**, *410* (6827), 450-453.
34. Kolluri, K.; Demkowicz, M. J., Coarsening by network restructuring in model nanoporous gold. *Acta Mater.* **2011**, *59* (20), 7645-7653.
35. Rosner, H.; Parida, S.; Kramer, D.; Volkert, C. A.; Weissmuller, J., Reconstructing a nanoporous metal in three dimensions: An electron tomography study of dealloyed gold leaf. *Adv. Eng. Mater.* **2007**, *9* (7), 535-541.
36. Sun, Y.; Balk, T. J., A multi-step dealloying method to produce nanoporous gold with no volume change and minimal cracking. *Scr. Mater.* **2008**, *58* (9), 727-730.
37. (a) Okman, O.; Lee, D.; Kysar, J. W., Fabrication of crack-free nanoporous gold blanket thin films by potentiostatic dealloying. *Scr. Mater.* **2010**, *63* (10), 1005-1008; (b) Jin, H. J.; Parida, S.; Kramer, D.; Weissmuller, J., Sign-inverted surface stress-charge response in nanoporous gold. *Surf. Sci.* **2008**, *602* (23), 3588-3594.
38. Snyder, J.; Livi, K.; Erlebacher, J., Dealloying silver/gold alloys in neutral silver nitrate solution: Porosity evolution, surface composition, and surface oxides. *J. Electrochem. Soc.* **2008**, *155* (8), C464-C473.
39. Okman, O.; Kysar, J. W., Fabrication of crack-free blanket nanoporous gold thin films by galvanostatic dealloying. *J. Alloy. Compd.* **2011**, *509* (22), 6374-6381.
40. Cattarin, S.; Kramer, D.; Lui, A.; Musiani, M. M., Preparation and characterization of gold nanostructures of controlled dimension by electrochemical techniques. *J. Phys. Chem. C* **2007**, *111* (34), 12643-12649.
41. Hammer, B.; Norskov, J. K., WHY GOLD IS THE NOBLEST OF ALL THE METALS. *Nature* **1995**, *376* (6537), 238-240.
42. Bond, G. C.; Sermon, P. A.; Webb, G.; Buchanan, D. A.; Wells, P. B., HYDROGENATION OVER SUPPORTED GOLD CATALYSTS. *J. Chem. Soc.-Chem. Commun.* **1973**, (13), 444-445.
43. Haruta, M.; Kobayashi, T.; Sano, H.; Yamada, N., NOVEL GOLD CATALYSTS FOR THE OXIDATION OF CARBON-MONOXIDE AT A TEMPERATURE FAR BELOW 0-DEGREES-C. *Chemistry Letters* **1987**, *16* (2), 405-408.
44. Hutchings, G. J., Vapor phase hydrochlorination of acetylene: Correlation of catalytic activity of supported metal chloride catalysts. *J. Catal.* **1985**, *96* (1), 292-295.
45. (a) Haruta, M., Size- and support-dependency in the catalysis of gold. *Catal. Today* **1997**, *36* (1), 153-166; (b) Bond, G. C.; Thompson, D. T., Catalysis by gold. *Catal. Rev.-Sci. Eng.* **1999**, *41* (3-4), 319-388.
46. Zielasek, V.; Jürgens, B.; Schulz, C.; Biener, J.; Biener, M. M.; Hamza, A. V.; Bäumer, M., Gold catalysts: Nanoporous gold foams. *Angew. Chem.-Int. Edit.* **2006**, *45* (48), 8241-8244.
47. Xu, C. X.; Su, J. X.; Xu, X. H.; Liu, P. P.; Zhao, H. J.; Tian, F.; Ding, Y., Low temperature CO oxidation over unsupported nanoporous gold. *J. Am. Chem. Soc.* **2007**, *129* (1), 42-43.
48. Xu, C.; Xu, X.; Su, J.; Ding, Y., Research on unsupported nanoporous gold catalyst for CO oxidation. *J. Catal.* **2007**, *252* (2), 243-248.

49. Wittstock, A.; Neumann, B.; Schaefer, A.; Dumbuya, K.; Kübel, C.; Biener, M. M.; Zielasek, V.; Steinrück, H.-P.; Gottfried, J. M.; Biener, J.; Hamza, A.; Bäumer, M., Nanoporous Au: An Unsupported Pure Gold Catalyst? *J. Phys. Chem. C* **2009**, *113* (14), 5593-5600.
50. (a) Wittstock, A.; Wichmann, A.; Biener, J.; Bäumer, M., Nanoporous gold: a new gold catalyst with tunable properties. *Faraday Disc* **2011**; (b) Fajin, J. L. C.; Cordeiro, M.; Gomes, J. R. B., On the theoretical understanding of the unexpected O(2) activation by nanoporous gold. *Chem. Commun.* **2011**, 47 (29), 8403-8405.
51. Asao, N.; Ishikawa, Y.; Hatakeyama, N.; Menggenbateer; Yamamoto, Y.; Chen, M. W.; Zhang, W.; Inoue, A., Nanostructured Materials as Catalysts: Nanoporous-Gold-Catalyzed Oxidation of Organosilanes with Water. *Angew. Chem.-Int. Edit.* **2010**, *49* (52), 10093-10095.
52. Christensen, C. H.; Norskov, J. K., Green Gold Catalysis. *Science* **2010**, *327* (5963), 278-279.
53. (a) Kosuda, K. M.; Wittstock, A.; Friend, C. M.; Bäumer, M., Oxygen-Mediated Coupling of Alcohols over Nanoporous Gold Catalysts at Ambient Pressures. *Angewandte Chemie International Edition* **2012**, n/a-n/a; (b) Xu, B.; Haubrich, J.; Freyschlag, C. G.; Madix, R. J.; Friend, C. M., Oxygen-assisted cross-coupling of methanol with alkyl alcohols on metallic gold. *Chem. Sci.* **2010**, *1* (3), 310-314; (c) Xu, B.; Madix, R. J.; Friend, C. M., Achieving Optimum Selectivity in Oxygen Assisted Alcohol Cross-Coupling on Gold. *J. Am. Chem. Soc.* **2010**, *132* (46), 16571-16580; (d) Xu, B.; Liu, X.; Haubrich, J.; Madix, R. J.; Friend, C. M., Selectivity Control in Gold-Mediated Esterification of Methanol. *Angew. Chem.-Int. Edit.* **2009**, *48* (23), 4206-4209; (e) Liu, X.; Xu, B.; Haubrich, J.; Madix, R. J.; Friend, C. M., Surface-Mediated Self-Coupling of Ethanol on Gold. *J. Am. Chem. Soc.* **2009**, *131* (16), 5757-5759.
54. Baker, T. A.; Liu, X.; Friend, C. M., The mystery of gold's chemical activity: local bonding, morphology and reactivity of atomic oxygen. *Phys. Chem. Chem. Phys.* **2011**, *13* (1), 34-46.
55. Han, D. Q.; Xu, T. T.; Su, J. X.; Xu, X. H.; Ding, Y., Gas-Phase Selective Oxidation of Benzyl Alcohol to Benzaldehyde with Molecular Oxygen over Unsupported Nanoporous Gold. *ChemCatChem* **2010**, *2* (4), 383-386.
56. Yin, H. M.; Zhou, C. Q.; Xu, C. X.; Liu, P. P.; Xu, X. H.; Ding, Y., Aerobic oxidation of D-glucose on support-free nanoporous gold. *J. Phys. Chem. C* **2008**, *112* (26), 9673-9678.
57. King, J. S.; Wittstock, A.; Biener, J.; Kucheyev, S. O.; Wang, Y. M.; Baumann, T. F.; Giri, S. K.; Hamza, A. V.; Bäumer, M.; Bent, S. F., Ultralow loading Pt nanocatalysts prepared by atomic layer deposition on carbon aerogels. *Nano Lett.* **2008**, *8* (8), 2405-2409.
58. Ding, Y.; Chen, M. W.; Erlebacher, J., Metallic mesoporous nanocomposites for electrocatalysis. *J. Am. Chem. Soc.* **2004**, *126* (22), 6876-6877.
59. Mathur, A.; Erlebacher, J., Effects of substrate shape, curvature and roughness on thin heteroepitaxial films of Pt on Au(111). *Surf. Sci.* **2008**, *602* (17), 2863-2875.
60. Herrero, E.; Buller, L. J.; Abruna, H. D., Underpotential deposition at single crystal surfaces of Au, Pt, Ag and other materials. *Chem. Rev.* **2001**, *101* (7), 1897-1930.
61. (a) Liu, Y. F.; Krug, K.; Lin, P. C.; Chiu, Y. D.; Dow, W. P.; Yau, S. L.; Lee, Y. L., In Situ STM Study of Cu Electrodeposition on TBPS-Modified Au(111) Electrodes. *J. Electrochem. Soc.* **2012**, *159* (2), D84-D90; (b) Trasatti, S.; Petrii, O. A., REAL SURFACE-AREA MEASUREMENTS IN ELECTROCHEMISTRY. *Pure Appl. Chem.* **1991**, *63* (5), 711-734.
62. Huang, J. F., Facile preparation of an ultrathin nickel film coated nanoporous gold electrode with the unique catalytic activity to oxidation of glucose. *Chem. Commun.* **2009**, (10), 1270-1272.
63. Rettew, R. E.; Guthrie, J. W.; Alamgir, F. M., Layer-by-Layer Pt Growth on Polycrystalline Au: Surface-Limited Redox Replacement of Overpotentially Deposited Ni Monolayers. *J. Electrochem. Soc.* **2009**, *156* (11), D513-D516.
64. Wichmann, A.; Wittstock, A.; Bäumer, M., *unpublished results* **2011**.
65. Steele, B. C. H.; Heinzl, A., Materials for fuel-cell technologies. *Nature* **2001**, *414* (6861), 345-352.

66. Rolison, D. R.; Long, R. W.; Lytle, J. C.; Fischer, A. E.; Rhodes, C. P.; McEvoy, T. M.; Bourga, M. E.; Lubers, A. M., Multifunctional 3D nanoarchitectures for energy storage and conversion. *Chem. Soc. Rev.* **2009**, *38* (1), 226-252.
67. Fiedler, E.; Grossmann, G.; Kersebohm, D. B.; Weiss, G.; Witte, C., Methanol. In *Ullmann's Encyclopedia of Industrial Chemistry*, Wiley-VCH Verlag GmbH & Co. KGaA: Weinheim, 2000.
68. Lang, X. Y.; Yuan, H. T.; Iwasa, Y.; Chen, M. W., Three-dimensional nanoporous gold for electrochemical supercapacitors. *Scr. Mater.* **2011**, *64* (9), 923-926.
69. Zhang, J. T.; Ma, H. Y.; Zhang, D. J.; Liu, P. P.; Tian, F.; Ding, Y., Electrocatalytic activity of bimetallic platinum-gold catalysts fabricated based on nanoporous gold. *Phys. Chem. Chem. Phys.* **2008**, *10* (22), 3250-3255.
70. (a) Lang, X. Y.; Qian, L. H.; Guan, P. F.; Zi, J. A.; Chen, M. W., Localized surface plasmon resonance of nanoporous gold. *Appl. Phys. Lett.* **2011**, *98* (9); (b) Kudo, A.; Fujita, T.; Lang, X. Y.; Chen, L. Y.; Chen, M. W., Enhanced Electrochemical Performances of Nanoporous Gold by Surface Modification of Titanium Dioxide Nanoparticles. *Mater. Trans.* **2010**, *51* (9), 1566-1569.
71. Reutemann, W.; Kieczka, H., Formic Acid. In *Ullmann's Encyclopedia of Industrial Chemistry*, Wiley-VCH Verlag GmbH & Co. KGaA: Weinheim, 2000.
72. Chen, Y. X.; Heinen, M.; Jusys, Z.; Behm, R. J., Kinetics and mechanism of the electrooxidation of formic acid - Spectroelectrochemical studies in a flow cell. *Angew. Chem.-Int. Edit.* **2006**, *45* (6), 981-985.
73. Wang, R. Y.; Wang, C.; Cai, W. B.; Ding, Y., Ultralow-Platinum-Loading High-Performance Nanoporous Electrocatalysts with Nanoengineered Surface Structures. *Adv. Mater.* **2010**, *22* (16), 1845-+.
74. Wang, R. Y.; Wang, C.; Cai, W. B.; Ding, Y., Ultralow-Platinum-Loading High-Performance Nanoporous Electrocatalysts with Nanoengineered Surface Structures. *Adv. Mater.* **2010**, *22* (16), 1845.
75. (a) Bai, Y.; Yang, W. W.; Sun, Y.; Sun, C. Q., Enzyme-free glucose sensor based on a three-dimensional gold film electrode. *Sensors and Actuators B-Chemical* **2008**, *134* (2), 471-476; (b) Qiu, H.; Huang, X., Effects of Pt decoration on the electrocatalytic activity of nanoporous gold electrode toward glucose and its potential application for constructing a nonenzymatic glucose sensor. *J. Electroanal. Chem.* **2010**, *643* (1-2), 39-45.
76. Qiu, H.-J.; Zhou, G.-P.; Ji, G.-L.; Zhang, Y.; Huang, X.-R.; Ding, Y., A novel nanoporous gold modified electrode for the selective determination of dopamine in the presence of ascorbic acid. *Colloids and Surfaces B: Biointerfaces* **2009**, *69* (1), 105-108.
77. Zeis, R.; Lei, T.; Sieradzki, K.; Snyder, J.; Erlebacher, J., Catalytic reduction of oxygen and hydrogen peroxide by nanoporous gold. *J. Catal.* **2008**, *253* (1), 132-138.
78. Qiu, H. J.; Xue, L. Y.; Ji, G. L.; Zhou, G. P.; Huang, X. R.; Qu, Y. B.; Gao, P. J., Enzyme-modified nanoporous gold-based electrochemical biosensors. *Biosens Bioelectron* **2009**, *24* (10), 3014-3018.
79. Wilson, R.; Turner, A. P. F., Glucose oxidase: an ideal enzyme. *Biosensors and Bioelectronics* **1992**, *7* (3), 165-185.
80. (a) Tominaga, M.; Taema, Y.; Taniguchi, I., Electrocatalytic glucose oxidation at bimetallic gold-copper nanoparticle-modified carbon electrodes in alkaline solution. *J. Electroanal. Chem.* **2008**, *624* (1-2), 1-8; (b) Vassilyev, Y. B.; Khazova, O. A.; Nikolaeva, N. N., KINETICS AND MECHANISM OF GLUCOSE ELECTROOXIDATION ON DIFFERENT ELECTRODE-CATALYSTS .1. ADSORPTION AND OXIDATION ON PLATINUM. *J. Electroanal. Chem.* **1985**, *196* (1), 105-125.
81. Tominaga, M.; Shimazoe, T.; Nagashima, M.; Taniguchi, I., Electrocatalytic oxidation of glucose at gold nanoparticle-modified carbon electrodes in alkaline and neutral solutions. *Electrochem. Commun.* **2005**, *7* (2), 189-193.



82. (a) Tominaga, M.; Nagashima, M.; Nishiyama, K.; Taniguchi, I., Surface poisoning during electrocatalytic monosaccharide oxidation reactions at gold electrodes in alkaline medium. *Electrochem. Commun.* **2007**, *9* (8), 1892-1898; (b) Tominaga, M.; Shimazoe, T.; Nagashima, M.; Kusuda, H.; Kubo, A.; Kuwahara, Y.; Taniguchi, I., Electrocatalytic oxidation of glucose at gold-silver alloy, silver and gold nanoparticles in an alkaline solution. *J. Electroanal. Chem.* **2006**, *590* (1), 37-46.
83. (a) Shulga, O. V.; Zhou, D.; Demchenko, A. V.; Stine, K. J., Detection of free prostate specific antigen (fPSA) on a nanoporous gold platform. *Analyst* **2008**, *133* (3), 319-322; (b) Shulga, O. V.; Jefferson, K.; Khan, A. R.; D'Souza, V. T.; Liu, J. Y.; Demchenko, A. V.; Stine, K. J., Preparation and characterization of porous gold and its application as a platform for immobilization of acetylcholine esterase. *Chem. Mat.* **2007**, *19* (16), 3902-3911; (c) Qiu, H. J.; Xu, C. X.; Huang, X. R.; Ding, Y.; Qu, Y. B.; Gao, P. J., Adsorption of laccase on the surface of nanoporous gold and the direct electron transfer between them. *J. Phys. Chem. C* **2008**, *112* (38), 14781-14785; (d) Qiu, H. J.; Xu, C. X.; Ji, G. L.; Huang, X. R.; Han, S. H.; Ding, Y.; Qu, Y. B., Immobilization of Laccase on Nanoporous Gold and Its Enzymatic Properties. *Acta Chim. Sin.* **2008**, *66* (18), 2075-2080; (e) Qiu, H. J.; Xu, C. X.; Huang, X. R.; Ding, Y.; Qu, Y. B.; Gao, P. J., Immobilization of Laccase on Nanoporous Gold: Comparative Studies on the Immobilization Strategies and the Particle Size Effects. *J. Phys. Chem. C* **2009**, *113* (6), 2521-2525.
84. Zhu, A.; Tian, Y.; Liu, H.; Luo, Y., Nanoporous gold film encapsulating cytochrome c for the fabrication of a H<sub>2</sub>O<sub>2</sub> biosensor. *Biomaterials* **2009**, *30* (18), 3183-3188.
85. Wei, Q.; Zhao, Y. F.; Xu, C. X.; Wu, D.; Cai, Y. Y.; He, J.; Li, H.; Du, B.; Yang, M. H., Nanoporous gold film based immunosensor for label-free detection of cancer biomarker. *Biosens. Bioelectron.* **2011**, *26* (8), 3714-3718.
86. Freyschlag, C. G.; Madix, R. J., Precious metal magic: catalytic wizardry. *Mater. Today* **2011**, *14* (4), 134-142.
87. (a) Prime, K. L.; Whitesides, G. M., SELF-ASSEMBLED ORGANIC MONOLAYERS - MODEL SYSTEMS FOR STUDYING ADSORPTION OF PROTEINS AT SURFACES. *Science* **1991**, *252* (5009), 1164-1167; (b) Prime, K. L.; Whitesides, G. M., ADSORPTION OF PROTEINS ONTO SURFACES CONTAINING END-ATTACHED OLIGO(ETHYLENE OXIDE) - A MODEL SYSTEM USING SELF-ASSEMBLED MONOLAYERS. *J. Am. Chem. Soc.* **1993**, *115* (23), 10714-10721.
88. Rostovtsev, V. V.; Green, L. G.; Fokin, V. V.; Sharpless, K. B., A stepwise Huisgen cycloaddition process: Copper(I)-catalyzed regioselective "ligation" of azides and terminal alkynes. *Angew Chem Int Edit* **2002**, *41* (14), 2596-+.
89. Zhu, A. W.; Tian, Y.; Liu, H. Q.; Luo, Y. P., Nanoporous gold film encapsulating cytochrome c for the fabrication of a H<sub>2</sub>O<sub>2</sub> biosensor. *Biomaterials* **2009**, *30* (18), 3183-3188.
90. Hashmi, A. S. K.; Hutchings, G. J., Gold catalysis. *Angew. Chem.-Int. Edit.* **2006**, *45* (47), 7896-7936.
91. Biener, M. M.; Biener, J.; Wichmann, A.; Wittstock, A.; Baumann, T. F.; Bäumer, M.; Hamza, A. V., ALD Functionalized Nanoporous Gold: Thermal Stability, Mechanical Properties, and Catalytic Activity. *Nano Lett.* **2011**, *11* (8), 3085-3090.
92. Kucheyev, S. O.; Biener, J.; Baumann, T. F.; Wang, Y. M.; Hamza, A. V.; Li, Z.; Lee, D. K.; Gordon, R. G., Mechanisms of atomic layer deposition on substrates with ultrahigh aspect ratios. *Langmuir* **2008**, *24* (3), 943-948.
93. Quiller, R. G.; Baker, T. A.; Deng, X.; Colling, M. E.; Min, B. K.; Friend, C. M., Transient hydroxyl formation from water on oxygen-covered Au(111). *J. Chem. Phys.* **2008**, *129* (6), 9.
94. Feng, Q.; Wen, P. H.; Tao, Z. Q.; Ishikawa, Y.; Itoh, H., Dye-sensitized solar cells based on anatase TiO<sub>2</sub> nanocrystals exposing a specific lattice plane on the surface. *Applied Physics Letters* **2010**, *97* (13).
95. Diebold, U., The surface science of titanium dioxide. *Surf. Sci. Rep.* **2003**, *48* (5-8), 53-229.

96. Green, I. X.; Tang, W.; Neurock, M.; Yates, J. T., Spectroscopic Observation of Dual Catalytic Sites During Oxidation of CO on a Au/TiO<sub>2</sub> Catalyst. *Science* **2011**, *333* (6043), 736-739.
97. (a) Rodriguez, J. A.; Hrbek, J., Inverse oxide/metal catalysts: A versatile approach for activity tests and mechanistic studies. *Surf. Sci.* **2010**, *604* (3-4), 241-244; (b) Rodriguez, J. A.; Liu, R.; Hrbek, J.; Perez, M.; Evans, J., Water-gas shift activity of Au and Cu nanoparticles supported on molybdenum oxides. *J. Mol. Catal. A-Chem.* **2008**, *281* (1-2), 59-65; (c) Rodriguez, J. A.; Ma, S.; Liu, P.; Hrbek, J.; Evans, J.; Perez, M., Activity of CeO<sub>x</sub> and TiO<sub>x</sub> nanoparticles grown on Au(111) in the water-gas shift reaction. *Science* **2007**, *318* (5857), 1757-1760.